Aus der Klinik für Neurologie mit experimenteller Neurologie
der Medizinischen Fakultät Charité – Universitätsmedizin Berlin

DISSERTATION

A study of the effects of antiepileptic drugs on the focal freeze lesion model: new insights on the pathophysiology of malformations of cortical development.

Auswirkungen von Antiepileptika auf das fokale Freeze-Läsionsmodell: neue Erkenntnisse zur Pathophysiologie von Malformationen kortikaler Entwicklung

zur Erlangung des akademischen Grades
Doctor of Philosophy (PhD)

vorgelegt der Medizinischen Fakultät
Charité – Universitätsmedizin Berlin

Von
Aliénor Ragot

Datum der Promotion: 30. Juni 2024

Table of Contents

List of figures

List of abbreviations

4AP	4-aminopyridine
aCSF	artificial cerebrospinal fluid
AED	anti-epileptic drug
ATZ	acetazolamide
BBB	blood-brain barrier
BUM	bumetanide
d.i.r.s.	difference in rank sum
CBZ	carbamazepine
Ect	ectorhinal cortex
EX	embryonic day X (X days after fertilization)
EEG	electroencephalogram
FFLM	focal freeze lesion model
GABA	γ-Aminobutyric acid
KCC	potassium chloride cotransporter
LCM	lacosamide
NMDA	N-methyl-d-aspartate
NMDG	N-methyl-D-glucamine
MCD	malformation of cortical development
MRI	magnetic resonance imaging
NKCC1	sodium potassium chloride cotransporter 1
P0	post-natal day 0, date of birth
PMG	polymicrogyria

PX	post-natal day X
SLE	seizure-like event
SmS	somatosensory
WHO	World Health Organisation
ZNS	zonisamide

Abstract

Malformations of cortical development (MCD) can lead to difficult-to-treat epilepsy in children and adults. They are characterized by physical abnormal tissue in the neocortex; however, it is often the area surrounding this malformation that is hyperexcitable. Antiepileptic drugs can be used to reduce the frequency or severity of seizures, but they do not target the relying cause of the epilepsy, only symptoms. I studied the effect of established and newer antiepileptic drugs in a model of MCD: the focal freeze lesion model (FFLM), that reproduces some of the characteristics of microgyria which is a frequent form of MCD.

After noticing visually, a reduction in the volume of the hemisphere, I tested the hypothesis that the freeze lesion led to a wider reduction in brain size, using magnetic resonance imaging. I induced seizure-like events (SLE) using the potassium channel blocker 4 amino-pyridine. I located the onset site of SLE using electrophysiology combined with intrinsic optical imaging. This method also allowed to study the propagation of seizure-like event in the slice. The analysis of this data led to the identification of the onset site in the lesioned slices and in the two controls, contralateral side, and sham-lesioned animals. I also analysed the electrophysiological parameters of the SLE in the three groups. I performed experiments during which I bath applied one of five antiepileptic drugs (AEDs) of different generations with different targets, and I measured their impact on SLE duration, frequency, propagation, and onset-site.

I showed and quantified for the first time a reduction of the volume of the lesioned hemisphere in the FFLM, limited to the neocortex. This could indicate a further involvement of the “healthy” normo-typic neocortex in the pathology. I confirmed that the perilesional area is the site of the initiation of spontaneous seizures. Taken together, these results can influence the treatments of MCD, notably surgical as removing the abnormal tissue would not be sufficient to prevent further seizures.

In this work, I described the mode of actions of all five AEDs in this model, confirming or contradicting general knowledge on these molecules. I showed that the sodium channel blockers carbamazepine and lacosamide suppressed SLE in this model but not specifically in the lesioned slices. Zonisamide and acetazolamide which target respectively calcium channels and the carbonic anhydrase had more contrasted effects, reducing either the frequency or the propagation of SLE in the model. Both had no specific

effect on the lesioned slices though. These results indicated that these four drugs can be efficient in MCD but that they do not target the abnormal networks. I also analysed the modes of action of the antiepileptic drugs and described whether they acted by limiting the initiation of SLE or by reducing the propagation of SLE. These data can be of great clinical use and influence the choice of AED (or the combination) prescribed in patients.

Finally, I showed for the first time a specific effect of the sodium potassium chloride cotransporter 1 (NKCC1) blocker bumetanide in adult lesioned neocortex, when it had no effect in the controls. This result indicates the persistence of an immature cortical network in this model and is an important contribution to the current discussion on the use of NKCC1 blockers in the treatment of MCD. I discuss here the possible clinical implications of these results and their limitations.

Zusammenfassung

Malformationen der kortikalen Entwicklung (MCD) können bei Kindern sowie Erwachsenen zu schwer behandelbarer Epilepsie führen. Sie sind durch Gewebeanomalien im Neokortex erkennbar, wobei jedoch häufig das periläsionelle Gewebe übererregbar ist. Um die Häufigkeit oder Schwere von Anfällen zu verringen, werden Antiepileptika eingesetzt. Diese zielen aber nicht auf die eigentliche Ursache der Epilepsie ab, sondern nur auf das Symptom epileptischer Anfall. Ich habe die Wirkung von etablierten und neueren Antiepileptika in einem Modell der MCD untersucht, dem fokalen Freeze-Läsion Modell (FFLM). Dies bildet einige der Merkmale von Mikrogyrien, einer häufigen Form von MCD, nach. Im FFLM habe Ich untersucht und aufgezeigt, dass die Volumenreduktion in der läsioniellen Hemisphäre größer als der eigentliche Gewebeverlust ist, der bei der Nekrose durch die Kühlläsion auftritt. Dies könnte auf einen weiteren Einfluss des "gesunden" normotypischen Neokortex an der Pathologie hinweisen. Mit Hilfe elektrophysiologischer und intrinsischer optischer Signalaufzeichnungen bestätigte ich, dass die 4AP-induzierten Anfälle mehrheitlich im normotypischen periläsionellen Bereich begannen.

Unterschiedliche Antiepileptika wurden in diesem Modell getestet, um 1. zu untersuchen, ob eine oder mehrere der Substanzen eine spezifische Wirkung auf das Modell haben, und um 2. ihre Wirkungsweise in diesem Modell zu untersuchen. Insbesondere bin ich der Frage nachgegangen, ob die untersuchten Antiepileptika (AEDs) die Entstehung von anfallsartigen Ereignissen (SLE, für seizure-like events) unterdrücken oder die Ausbreitung von SLE reduzieren. Ich wählte etablierte und neuere AEDs mit unterschiedlichen vermuteten Zielstrukturen und Wirkungsweisen aus, die Natriumkanalblocker Carbamazepin und Lacosamid, den T-Typ-Kalziumkanalblocker Zonisamid, den potenten Karbonanhydraseblocker Acetazolamid und schließlich den Chlorid-Cotransporter NKCC1-Blocker Bumetanid.

Ich habe die Wirkungsweise aller fünf AEDs in diesem Modell beschrieben und damit das allgemeine Wissen über diese Moleküle bestätigt oder widerlegt. Carbamazepin und Lacosamid blockierten die SLE in allen Gruppen erfolgreich. Ihre Wirkung war nicht läsionsspezifisch. Zonisamid und Acetazolamid hatten intermediäre Wirkungen, indem sie die Häufigkeit oder Ausbreitung von SLE reduzierten, ohne sie vollständig zu blockieren, der Effekt war nicht läsionsspezifisch.

Bumetanid blockierte die SLE in diesem Modell spezifisch, was das anormale Vorhandensein von NKCC1 in diesem kortikalen Netzwerk adulter Nager aufzeigte. Der NKCC1 ist normalerweise nur in unreifen neuronalen Netzwerken vorhanden und beeinflusst E_{GABA} stark, indem er das GABA-Gleichgewicht in Richtung desdepolarisierenden GABA verschiebt. Diese Ergebnisse deuten auf das Fortbestehen eines unreifen Netzwerks in dem FFLM und damit auch bei MCD hin. Ich gehe in meiner Arbeit auf die möglichen klinischen Implikationen dieser Ergebnisse und ihre Limitationen ein.

1. Introduction

Around 50 million people worldwide suffer from epilepsy, one of the most prevalent neurological disorders (1). A cumulative study including data from 128 million people evaluated the global yearly incidence of epilepsy as more than 68 cases per 100 000 persons worldwide (2) the prevalence is 7 per 1,000 persons (3)

The disease is considered by the World Health Organization as one of the neurological disorders that causes the heaviest burden on affected patients as they have to deal with psychological, social, and cognitive consequences of the disease as well as the neurological symptoms (1). Although epilepsy is primarily characterized by the presence of epileptic seizures, all these aspects of the disease are now included in the updated definition of epilepsy by the International League Against Epilepsy (2014). The misconceptions and stigma around the disease can also impact the lives of patients greatly.

In most patients, seizures can be prevented, or their frequency can be significantly reduced by antiepileptic drugs (AEDs), however, almost a third of patients fail to respond to available therapies.

Malformation of cortical development (MCD) are related with hard-to-treat epilepsy in children and adults, as recent data from various Epilepsy centres still show (4–7).

MCD encompass a variety of pathologies defined by their clinical patterns and macroscopic anatomical defects identified by magnetic resonance imaging including focal cortical dysplasia, heterotopia, hemimegaencephaly, polymicrogyria (PMG) and others (8). These lesions are the consequence of one or several events occurring during cortical development. The development of the cortex or corticogenesis is a highly spatial- and time-sensitive sequence of processes which can be regrouped into four partially overlapping phases: progenitor division and neurogenesis, migration, neuritogenesis (extension of axon and dendrites) and synaptogenesis (9). Any disruption of this highly regulated processes can lead to MCD.

These malformations, in their most severe forms, can lead to a wide range of neurological clinical expressions: autistic spectrum disorders, intellectual disabilities, failure to reach developmental milestones and often epilepsy. The incidence of epilepsy is notably

remarkably high in children with polymicrogyria, for which it was estimated that 80% of children will develop epilepsy within their first five years (10).

The pathological process leading from the visually defined malformations to seizure susceptibility is however still unclear.

1.1 The lack of complete understanding of the pathomechanisms limits the ability to treat efficiently all patients with epilepsy.

In the last decades, a large number of AEDs have been developed, some with new mechanisms of action, thus creating an almost infinite list of possible drug combination to try on patients (11). Nevertheless, most AEDs target the main symptom of epilepsy, the epileptic seizure, by preventing synchronous abnormal neuronal firing, but do not address the disease's underlying causes.

Even though they have superior pharmacokinetics and side effect profiles, the efficacy of the new AEDs is not greater than that of the previous generation of AEDs. A longitudinal study, conducted in the same health care centre in Scotland over 30 years, showed that the rate of seizure-free patients did not increase during the period, despite the introduction of various new AEDs (12).

In patients with drug-resistant epilepsy (for which at least two appropriately chosen AEDs, tolerated by the patient, have failed to achieve seizure freedom, ILAE’s definition 2010 Kwan et al., 2010b), the most effective course of action is often surgical resection of the epileptic focus i.e., the seizure onset zone (14). However, seizure freedom in patients with malformation of cortical development after surgery is difficult to achieve because the epileptogenic foci can be multiple, and they are more difficult to define with precision (15,16).

Even though some molecular targets have been identified for most AEDs used currently, the exact modes of action of AEDs are not well understood. It is especially interesting to study the pharmacodynamics of drug combinations from the perspective of mode of inhibition (17).

In broad lines, AEDs can prevent seizures from starting, by diminishing the hyperexcitability in the epileptogenic region, or they can limit the impact of the seizures

by decreasing the propagation of the epileptic activity to other brain structures. Some AEDs, however, appear to be able to do both, while other modes of action remain unclear.

The way to improve treatment in patients with difficult-to-treat epilepsies might be to refine the panel of AEDs offered to specific subsets of patients, and/or to suggest drug combinations based on a better comprehension of the pathomechanisms underlying epilepsy as well as a better understanding of the mode of action of AEDs.

1.2 The focal freeze lesion model

The focal freeze lesion model (FFLM), first described by Dvorak and Feit (18), offers the opportunity to investigate these mechanisms. In fact, the post-natal lesion replicates the histopathological features of human 4-layered polymicrogyria (19) and epileptiform events comparable to those observed in human adult cortical network can be induced.

In the neonatal FFLM, cold is applied to the surface of the scalp on the day of birth, which creates a necrosis area in the neocortex below. The immature cortical network locally destroyed by the cold, is quickly replaced by migrating neuroblasts. The new neurons form by P7-P8 a four layered structure resembling a microgyrus (20,21), as seen in patients with polymicrogyria. Eventually, field potential epileptiform activity is seen from P12 (22). This delay has some similarities with the latency observed before the development of epilepsy in MCD patients. In fact, the incidence of seizures in polymicrogyyria is high in children with PMG under 5 years, however epilepsy can also develop later, in adolescents and young adults (10,23,24).

However, this microgyrus-like lesion is not in itself epileptogenic. It has been shown that a series of increasingly intense stimuli, in deep neocortical layers, evokes epileptiform activity, specifically in the perilesional area (the normo-typic area directly surrounding the lesion). Contrarily, stimulations inside the microgyrus had no effect (25).

There is no scarcity of neurons in layers II–III of the microgyrus, according to earlier research on the FFLM (18,25), but there is a distinct reduction in the number of afferents going to these levels, as compared to control cortex (26). On the other hand, the perilesional area (around the lesion) is hyperinnervated by thalamo-cortical excitatory afferents (26,27) and callosal afferents (28). Additionally, it has been shown that cortical expression of the $GABA_A$ receptor subunits α1, α 2, α 3, α 5, and γ2 is significantly reduced (29). This downregulation could be to compensate for the increase in excitatory

drive on GABAergic neurons in the perilesional area (29). The combination of these changes would explain the perilesional area's greater excitability.

SLE can be evoked in the perilesional area by stimulation, but they are not observed in moving animals, and do not spontaneously occur (30). In some studies, spontaneous seizures in these rats were reported, but only after a second hit with hypothermia at P10 (31) .

This hyperexcitability of the perilesional area is maintained in adults where it reaches “a chronic state of hyperexcitability” in comparison to control mature neocortex were the excitability of low (32).

To study the point of origin of seizures in relation to the lesion, in the absence of stimulation, the threshold for occurrence of seizure-like events can be lowered in the whole slice, by bath application of 4 aminopyridine (4AP). 4AP creates an overall increase of excitability, therefore SLE occur regularly (33). This baseline of epileptic-like activity in the slices is necessary to study the mode of action of the AEDs.

The scope of the semiology, i.e., the clinical symptoms, of an epileptic seizure, is a direct consequence of the site of onset and of the extent of the seizure propagation in the brain.

1.3 The neurotransmitter GABA, role in cortical development and in the pathomechanism in MCD

GABA is the main inhibitory neurotransmitter in the adult brain.

Some of the oldest AEDs modulate GABAergic transmission to reduce the excitability of the network: benzodiazepines and barbiturates act on postsynaptic $GABA_A$ receptors (34).

In immature neurons, GABAergic transmission is depolarising (35) to promote neurogenesis. The excitability of the immature cells facilitates neuronal proliferation, migration, and synaptogenesis (36). At the end of the neurogenesis, a shift to hyperpolarization occurs gradually in different brain structures(37).

The shift in E_{GABA} is induced by a decrease in the intracellular chloride concentration, which is regulated by NKCC1 and KCC2 ion cotransporters. In the rat neocortex, NKCC1 mRNA expression is highest in the first day after birth and starts decreasing while KCC2

mRNA increases. (38–41). In humans, the pattern of expression is similar, but the shift happens during the embryonic period, at 35 weeks after conception (42).

The abnormal persistence of excitatory GABA function in adulthood has been suggested as a mechanism contributing to epileptogenesis (43), and was observed in patients with focal cortical dysplasia (44,45).

In the FFLM, NKCC1 is overexpressed in the days following the freeze-lesion, while KCC2 is downregulated (46), thus inducing $GABA_A$ receptor-mediated Ca^{2+} oscillation (47). At the end of the second week of birth after the microgyrus has been formed, the levels of expression of the cotransporters in the microgyrus were measured to be normal, (46).

Yet, the abnormal presence of radial glia in adult freeze-lesioned rats (48) and the maintained hyperexcitability in the perilesional area in adulthood (32) are elements in favour of the persistence of immature neocortical network in the perilesional area in adult rats.

1.4 Hypotheses

Whether an immature network persists in adult patients with MCD remains under debate, I therefore decided to test this hypothesis by measuring the effect of the NKCC1 blocker bumetanide in the FFLM of MCD in young adult animals.

I designed an experimental protocol that allowed the study of the effect of AEDs on the initiation and on the propagation of the seizure activity in a model of MCD.

Finally, I tested whether AEDs are efficient in reducing the ictal activity in this model and analyse if their mode of action involved a limitation of the initiation or/and a reduction of the propagation of seizure-like events. The AEDs selected were:

- two established sodium channel blockers with hypothesized different molecular targets: the second-generation AED carbamazepine and the third-generation AED lacosamide.

- the voltage-gated calcium channel blocker zonisamide

-the carbonic anhydrase blocker acetazolamide

- the NKCC1 blocker bumetanide

2. Methods

2.1 Ethical statement.

The experimental protocol was designed in accordance with the guidelines of the European Communities Council (2010/63/EU) relating to animal welfare and ethics of animal experimentation. We also obtained approval from the local animal welfare authority (Landesamt für Gesundheit und Soziales Berlin, approval no. G0107/14) for all experiments. As the experiments were conducted only on male pups, I collaborated with other researchers who included our female pups in their experiments whenever possible.

2.2 Focal freeze lesion model.

I used the postnatal freeze lesion method described by Dvorak and Feit (18) and later modified by Luhmann and Raabe (49) on male Wistar rat pups. I took the new-born rats away from the mother and placed them under infrared light prior to the procedure.

I divided the pups randomly into two groups: treatment and sham. The randomization process was carried out as follows: a naive person was asked to write down numbers for the treatment group. I read the list of the selected only after I had attributed a number to each pup.

I gave orally a drop of the analgesic Novalgin® (Sanofi-Aventis, Frankfurt Germany) to each pup and then put them under deep anesthesia by hypothermia. We chose this method of anesthesia for its high expected recovery rate in neonate rats.

After verifying the absence of paw withdrawal reflexes in the anesthetized pups, after disinfection (Aseptoderm®, Dr Schumacher GmbH, Malsfeld, Germany), I made a 3-4 mm longitudinal incision on the skin of the right hemisphere, at approximatively 2 mm lateral to the midline.

I applied a cylindrical copper rod (⌀ 2 mm), cooled down by liquid nitrogen, on the exposed scalp of the pup, in 3 consecutive positions, each for 10 s, thus creating a 3 mm long line on the rostro-caudal axis. I carried out the same procedure on the sham-operated group, except for the temperature of the rod which remained at room temperature. I then sutured immediately after applying the rod on the scalp, and closed the skin incision with tissue

glue (Histoacryl®, B.Braun, Melsungen, Germany). I returned the operated animals under the infrared light for recovery. Within 5 minutes, all pups were awake and active.

Then, I firstly cleaned the pups with water (to remove any blood, glue, and disinfectant smells), then I rubbed them with the mother faeces, before placing them back into the cage. These steps were done to limit the risk of rejection by the mother.

The procedure took between 40 and 120 min (depending on the size of the litter) during which the pups were away from the mother. I monitored the weight of the pups 5 times a week for two weeks after surgery. Later, I handled the animals around once a week to accustom them my presence before the experiments. In total, 104 Wistar Han rats, 39 sham-operated and 65 freeze-lesioned animals, were included in this study.

2.3 Magnetic resonance imaging.

I performed the MRI scan acquisition on young adult rats, at postnatal day 42 (treatment group: n=9; sham group: n=3). For the scan acquisition, each animal was placed under isoflurane anesthesia (3% isoflurane in 30% O2 / 70% N2O) and kept warm with a heated blanket into a rodent, inside a 7T-MRI Pharmascan 70/16 AS (Bruker BioSpin, Ettlingen, Germany). I recorded their respiration rates (Small Animal Monitoring & Gating System, SA Instruments, Stony Brook, New York, USA) and monitored it continuously during the image acquisition.

I acquired coronal T2 weighted scans of the whole brain with a Turbo-Spin Echo Sequence (TR/TE = 4200/36 ms, rare factor 8, 10 averages, 25 coronal slices, slice thickness 0.75 mm, field of view 3.2x3.2 cm, matrix size 256x256, scan time 16 min).

I analysed the scans using Analyze 10.0 software (Analysedirect, Inc.; Lenexa USA): I segmented brain areas (hemispheres, left and right hippocampi and neocortex) and calculated the volume of each area.

During the MRI acquisition, I noticed two animals from the lesioned group, with abnormally large brain damage. These two animals were excluded from the analysis.

2.4 Preparation of acute brain slices.

Treated and sham rats were sacrificed between the ages of 6 and 10 weeks by decapitation after being sedated with isoflurane (3% isoflurane in 100% oxygen). The

habituation by handling ensured that animals showed no signs of stress when I removed them from the cages and during anaesthesia. I promptly extracted the brains and put them in a carbogen-equilibrated (95% O2 and 5% CO2) cold slicing solution (NMDG-aCSF; see details in the "Solutions and medicines" section).

I made a cut to isolate each hemisphere and prepared 400 µm thick coronal slices with a vibratome (Leica VT1200S, Wetzlar, Germany). I moved the slices into a specially created Haas-type interface chamber kept at 35°C and superfused (at a volume flow of around 2 ml/min) them with oxygenated aCSF (prewarmed at 35°C, details in “Solutions and medicines”). Prior to recording, slices were given one hour to recuperate.

2.5 Electrophysiological recordings.

I filled two borosilicate glass micropipettes with 1 M NaCl (1.5 mm outer diameter, ~1 MΩ; Science Products GmbH, Hofheim, Germany) and placed them in layers II/III of the somatosensory (SmS) and ectorhinal cortex (Ect) to allow for the continuous acquisition of extracellular field potentials.

After amplification (100x) and 3 kHz low pass filtering by custom-designed amplifiers, the signals were digitized and displayed at 10 kHz per channel using a CEDmicro1401 interface and Spike7 software (Cambridge Instruments, Cambridge, UK).

To induce seizure-like events (SLE), I added the non-specific potassium channel blocker 4-aminopyridine (4AP, Sigma-Aldrich, Munich, Germany, 100 M) to the bath. The experimental protocol included three 60 min phases: “baseline recording”, “drug phase”, and “washout phase”), see Figure 1. After 45 min of induction, the frequency and duration of SLE reached a plateau. I therefore calculated baseline values during the last 15 min of the “baseline phase” and used the final 20 min of each phase to assess the effects of drug administration and washout.

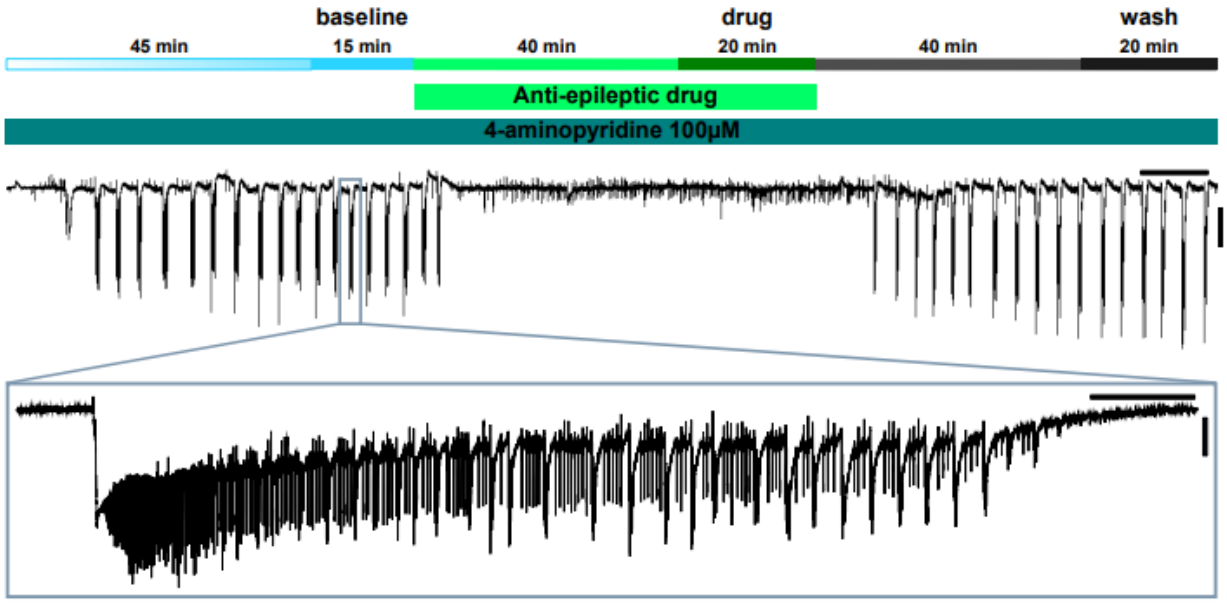

Figure 1 Experimental protocol for electrophysiological and IOS recordings. One experiment includes three phases of 60 min each. The darker rectangles at the end of each section indicate the period used for analysis of the phase. 4AP induces SLEs during the baseline phase, then the tested AED is applied for 60 min and washed out for another 60 min. Inset: one SLE defined by a sharp drop of the field potential followed by a tonic phase, then a clonic phase during which the frequency of ictal spikes decreases. Scale bars: 1 mV, 10 min; inset: 2 s (modified from Ragot et al., 2021).

2.6 Intrinsic optical signal recordings (IOS).

A CCD camera (VC1910, Sanyo, Tokyo, Japan) mounted on a binocular X16 microscope was used to capture optical signals (MS5, Leica, Wetzlar, Germany) during all electrophysiological recordings. In order to acquire intrinsic optical signals, I deposited the slices on a transparent membrane (0.4 µm Millicell® culture plate inserts; Millipore, Bedford MA, USA), and I placed a cold light source (KL 1500 Schott, Leica, Wetzlar, Germany) directly below the chamber.

With the use of a frame-grabber board (pciGrabber-4plus, Phytec, Mainz, Germany), 320x240-pixel images were produced from the 8-bit video signals. I analysed these pictures with a custom-made software and specially created ImageJ/FIJI macros. During the whole experimental protocol, a loop of 10 sec was constantly recorded (at roughly 10 Hz) using a circular data buffer. When an SLE was detected in the electrophysiological recordings, I manually began recording the optical signals. So, the sequence of images for each SLE includes a baseline of 100 pictures before the start of the event and approximately 500 pictures during the event itself.

I calculated a single image's light transmittance as a relative change (ΔT/T) from baseline transmittance (which is the average of the first 50 baseline images). For subsequent analysis, I split all neocortical areas into region of interests (ROI) that each measured 10x10 pixels. In each slice, the total number of ROIs varied according to the size, position, and shape of the slice.

Using ImageJ/FIJI and Matlab, I examined the light transmittance in each ROI separately (Version R2014b The MathWorks, Inc., Natick, Massachusetts, United States). I regarded changes that were less than 1% as noise and excluded them from the analysis. By identifying the first ROI in which an increase in light transmittance beyond threshold was measured, I identified the onset area for a specific SLE.

I then sorted the onset sites, using the Paxinos rat brain atlas (51), into the following five anatomical regions: motor, somatosensory (SmS), auditory (Aud), ectorhinal (Ect), and temporal (Temp) cortices. A second, naïve person was asked to place the limits of the areas on the picture of the slice, as control against a possible personal bias. I also performed a post-hoc analysis of the two following parameters: optical signal time course and maximum intensity during an event. These parameters were measured in the ROI with the greatest increase in light transmittance for this SLE.

I determined the size of area affected by the propagation of the SLE (in cm^2) by calculating the absolute number of ROIs with an IOS change greater than 1%. In case the drug tested fully blocked the SLE after 40 min of application, the affected area was calculated from the SLE occurring 15-35 minutes after application rather than 40-60 minutes after application.

2.7 Solutions and drugs.

The composition of the NMDG-aCSF used for slicing (52) was as follows (in mM): NMDG 93, KCl 2.5, NaH2PO4 1.2, NaHCO3 30, MgSO4 10, CaCl2 0.5, HEPES 20, glucose 25, Na-L-ascorbate 5, thiourea 2 and Na-pyruvate 3.

The aCSF used for storage of the slices and electrophysiological recordings was composed of (in mM): NaCl 129, NaH_2PO_4 1.25, $CaCl_2$ 1.6, KCl 3.0, $MgSO_4$ 1.8, $NaHCO_3$ 21 and glucose 10.

The concentrations of AED and of 4AP employed were based on earlier research (53–57).

The following drugs were bought from Sigma-Aldrich (Munich, Germany): 4AP (100 µM), bumetanide (10 µM), carbamazepine (50 µM), and acetazolamide (0.5 mM); while lacosamide (100 µM) came from Toronto Research Chemicals Inc. (Toronto, Canada) and zonisamide (100 µM) was purchased from Selleck Chemicals (Munich, Germany).

I prepared each AED into a stock solution, by using the suitable solvents: bumetanide, acetazolamide and zonisamide in dimethyl sulfoxide (DMSO) (<0.1% vol./vol. in final solution except for zonisamide with 0.2% DMSO); 4AP in bidistilled water; lacosamide in methanol (0.1% vol./vol.) and carbamazepine in ethanol (<0.1% vol./vol.)

2.8 Data analysis and statistics.

All data are given with arithmetic mean SD. I analysed the data using GraphPad Prism5 (GraphPad for Windows, GraphPad Software Inc., La Jolla, California, USA). I used non-parametric Kruskal-Wallis or Friedman tests (wherever relevant) to assess differences in SLE and IOS parameters between treatment groups, followed by Dunn post-hoc testing. I regarded P-values as significant below 0.05 (*p0.05; **p0.01; ***p0.001 for comparison to baseline and #p0.05 for comparison to washout).

3. Results

3.1 Establishment of the focal freeze lesion model

The protocol used for the FFLM led to a very low mortality rate (< 5 %) in the animals, with highest mortality (~3%) in the first week. The survival rate did not differ between sham operated and lesioned animals (50).

The freeze lesion produced consistently gyrus-like lesions in the right somato-sensory cortex (SmS) and no lesion was ever seen in the sham-operated group. However, during the establishment of the method, the brain damage produced in some animals was much larger and included parenchyma and subcortical areas despite following an identical protocol. These large lesions resembled the previously described “porencephalic cyst” observed in the FFLM (58) and resembled schizencephalic lesions (59). The animals with such defects (n=14), were excluded from the study and I precisely defined the shape and size of the lesion: only animals with a four-layer microgyrus-like lesion not wider than 2 mm were included in the study. Abnormal lesions were never seen after the fourth surgery. The experience of the experimenter appears to be a critical factor to obtain a

microgyrus-like lesion as the protocol remained identical across the study. It is also possible that the animals with the larger lesions, had been a few hours older than their siblings (as most births occurred at night, the exact time of birth of each pup was not monitored).

3.2 The hemisphere on the side of the lesion is smaller than expected

During the preparation of acute brain slices, I noticed that the lesioned hemisphere appeared systematically smaller than the contralateral. The analysis of MRI T2 weighted scans confirmed the visual assessment. The lesioned hemisphere is 9.0 +/- SD 3.9% smaller than the contralateral one whereas there is no difference in hemisphere volume in the sham animals (1.0 +/- SD 1.2%); these two ratios are significantly different (Mann Whitney test, two-tailed P value 0.0167), see Figure 2. Further analysis of the scans showed that the reduction of volume is limited to the neocortex and hippocampal volumes were not affected.

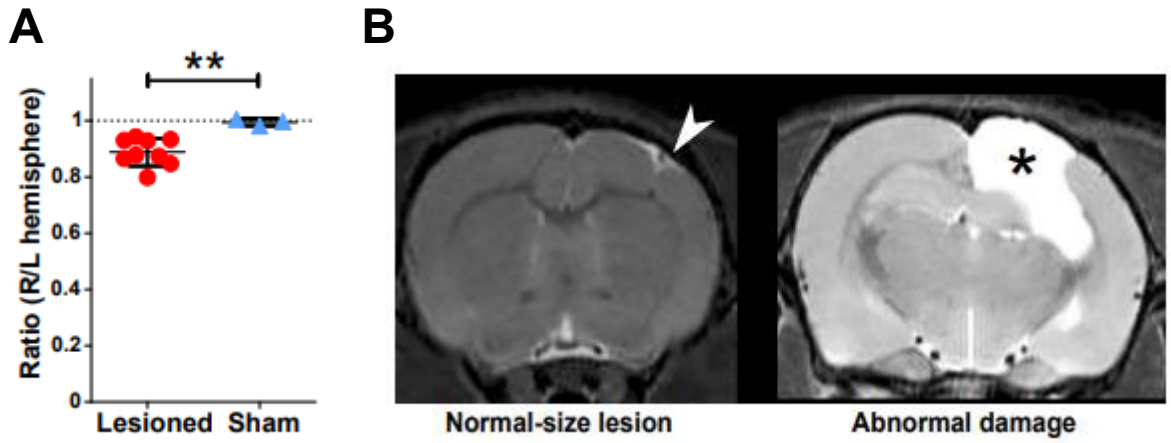

Figure 2 The lesioned hemisphere is smaller than the contralateral. A. Ratio of the volume of the hemispheres measured on T2 scans and shown as right-to-left ratio (9 rats, 0.89 ± 0.05) vs. sham operated rats (3 rats, 1.00 ± 0.02) (**, $p < 0.01$, non-parametric t-test), the freeze-lesion was down on the right hemisphere. B. Coronal MRI scans (T2) of two lesioned animals: on the left, "normal" microgyrus (white arrowhead in left image); on the right, abnormal damage of cortical and subcortical parenchyma (asterisk in right image), discarded from analysis (modified from Ragot et al., 2021).

3.3 The parameters of the SLEs do not differ between focal freeze lesion and control slices.

The bath application of the K^+ channel blocker 4AP invariably induced SLE consisting in an initial depolarization ("DC shift") followed by a tonic-like and a clonic-like phase, in

acute coronal slices. The SLE lasted around 40 seconds during which the event propagated laterally in the neocortex.

Upon wash in of 4AP, the duration of SLE increased to reach a plateau after 40 min of application. The epileptiform activity remained then stable for 4h (frequency and duration of the events). Considering that 4AP was bath applied, the SLEs started “spontaneously” in all areas of the neocortex, however field potentials were recorded in the SmS – where the lesion is located - and in the Ect cortex – distant from the lesion.

None of the intrinsic properties of the SLE such as duration, spike frequency and number of spikes per event differed between the lesioned slices, the contralateral slices and the slices from the sham animals. The inter-event interval and the number of events during plateau were also similar in all three groups.

Finally, the parameters of the SLE propagation: intensity of the IOS as well as the size of the area affected by the SLE showed no difference between the groups.

3.4 The onset site of SLE is the perilesional area

The IOS analysis led to the identification the onset site of each SLE.

The SLE started in all areas of the neocortex in all groups, yet in the lesioned slices the majority of SLE started in the SmS, where the lesion is located (Kruskal-Wallis test – 5 groups; KW statistic 33.23; P value < 0.0001 and Dunn’s multiple comparison test).

In the sham, the SLE started as frequently in the neighbouring area Aud as in the SmS (Kruskal-Wallis test – 5 groups; KW statistic 14.60; P value < 0.01 and Dunn’s multiple comparison test). Similarly in the contralateral slices, the onset sites were as frequently in the SmS, the Aud or the Ect (Kruskal-Wallis test – 5 groups; KW statistic 19.14; P value <0.001 and Dunn’s multiple comparison test).

The mean position of the onset site, in relation to the center of the microgyria, was calculated for each animal. In the lesioned slices, the onset site is located in the neocortex at a distance of 1.8mm +/- 0.3mm from the center of the microgyrus (and all SLE started in the layers II-III). I defined this area, adjacent to the microgyrus (1.5 - 2.5 mm from the center of the microgyrus) and comprised of normo-typical neocortex (6 layers, normal thickness) as the perilesional area.

The probability for SLE to occur is higher in the perilesional area than in the rest of the neocortex suggesting that the reorganization of the cortical network after the freeze-lesioning renders this area more prone to seizure-like activity.

3.5 Bumetanide has an antiepileptic effect in the lesioned hemisphere only

I tested the effect of bumetanide (BUM) at a concentration for which it is specific for NKCC1 (10µM).

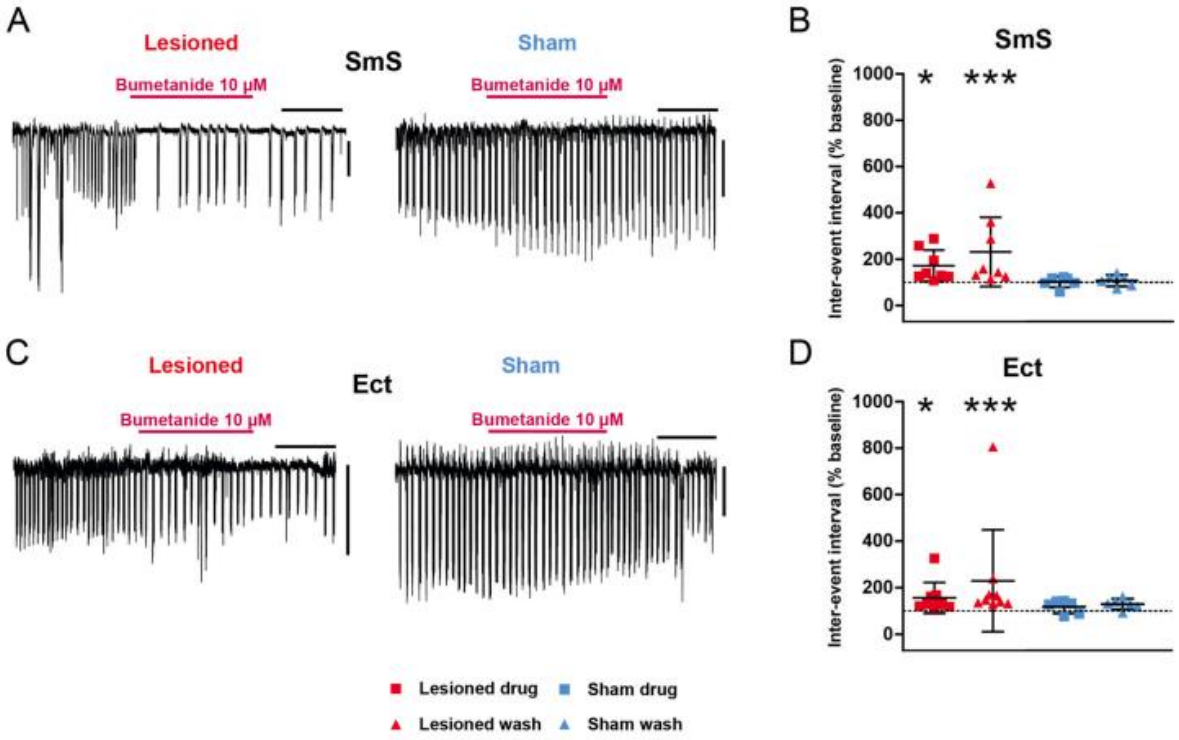

Figure 3 Lesion-specific reduction of seizure-like events by NKCC1 blocker bumetanide. (A, C) Representative traces of the effect of bumetanide on 4-AP induced SLEs in SmS (A) and Ect (C) in lesioned (left) and sham (right) animals. Pink lines indicate bumetanide application. Bumetanide has no effect on SLE in the sham group. (B, D) SLE inter-event intervals (expressed as % of baseline) for individual recordings in SmS close to the lesion (B SmS; lesioned drug: 170.8 ± 68.5%, lesioned wash: 231.0 ± 149.5%, sham drug: 101.5 ± 23.4%, sham wash: 107.1 ± 24.8%) and Ect (D lesioned drug: 155.8 ± 66.3%, lesioned wash: 229.6 ± 218.9%, sham drug: 118.0 ± 28.5%, sham wash: 129.5 ± 22.9%) after wash in of bumetanide 10µM. Means and SD indicated by lines. Scale bars: 2 mV, 30 min. Dashed lines in (B) and (D) mark the 100% threshold (modified from Ragot et al., 2021).

In the lesioned slices, bumetanide increased significantly the inter-event interval in the SmS to 170.8 % +/- 68.5 % (mean +/- SD in percentage of the baseline). The inter-event interval kept increasing during wash to 231% +/- 149.5 % (Friedman test comparing

baseline-BUM-wash for lesioned slices in SmS: 14.0, p<0.0001, and Dunn's multiple comparison test baseline vs BUM diff in rank sum or d.i.r.s. -9.50, p<0.05; baseline vs wash -14.5, p<0.001 in SmS), see Figure 3.

A similar increase in the inter-event interval was recorded in the Ect cortex of lesioned slices (Friedman test comparing baseline-bum-wash for lesioned slices in Ect: 14.25, p<0.0001, and Dunn's Multiple Comparison Test baseline vs BUM diff in rank sum -9.00, p<0.05; baseline vs wash -15.0, p<0.001 in Ect).

To the contrary, bumetanide had no effect on the inter-event interval in either the contralateral slices or the sham (Friedman test comparing baseline-BUM-wash, in the SmS respectively: 4.00, p=0.149 and 1.34, p=0.571; in the Ect respectively: 1.75, p=0.531 and 4.34, p= 0.142).

The size of the area affected by the SLE is not affected by bumetanide in any of the groups, so the mechanism of propagation of the SLE are not impacted by bumetanide (Friedman test comparing baseline-BUM-wash lesioned Friedman statistic 2.18, p=0.329; sham FS 2.70, p=0.252; contralateral FS 3.68, p=0.149).

The intensity of the IOS is diminished by bumetanide application in the lesioned slices only (Friedman test comparing baseline-BUM-wash: lesioned FS 15.9, p<0.0001 and Dunn's Multiple Comparison test baseline vs drug: difference in rank sum 10.5, p<0.05 and baseline vs wash d.i.r.s. 16.5, p<0.01; sham FS 4.96, p=0.072; contralateral FS 4.71, p=0.120).

Since there was a specific effect of bumetanide on the lesioned slices compared to both controls, I investigated whether the onset site of SLE in the lesioned slices is affected by bumetanide.

When bumetanide is applied, the onset site of SLE shifts away from the lesion (Friedman test comparing baseline-bum-wash in lesioned slices Friedman statistic 8.000, p=0.0162 and Dunn's Multiple Comparison Test baseline vs BUM -10.00, p<0.05; baseline vs wash -2, ns).

3.6 The sodium channel blockers have an antiepileptic effect, independent of the lesion.

In contrast to bumetanide, the sodium channels blockers carbamazepine (CBZ) and lacosamide (LCM) did not affect the lesioned slices differently from the controls. Both

these sodium channel blockers have a very strong effect on the 4AP induced SLE in all three groups.

The inter-event interval is drastically increased upon carbamazepine application in all groups (Friedman test in **lesioned** FS = 8.40, $p < 0.01$ and Dunn's Multiple Comparison test: baseline vs CBZ diff. in rank sum -9.00, $p<0.001$ and CBZ vs wash diff. in rank sum 6.00, ns; **sham** FS = 11.47, $p< 0.01$ and Dunn's multiple comparison test: bas. vs CBZ d.i.r.s. -13.0, $p<0.01$, and CBZ vs wash d.i.r.s. 8.00, ns; and **contralateral** FS = 13.61, $p<0.0001$ and Dunn's multiple comparison test: baseline vs CBZ d.i.r.s. -14.5, $p<0.001$, and CBZ vs wash d.i.r.s 8.00, ns).

The size of the area affected by the SLE is not significantly affected by carbamazepine in the controls (Friedman test in **sham** FS = 3.63, $p = 0.192$; and **contralateral** FS = 4.75, $p = 0.12$). In opposition carbamazepine appears to reduce the size of the area in the lesioned slices (**lesioned** FS = 7.68, $p < 0,01$ and Dunn's multiple comparison test: baseline vs CBZ diff in rank sum 8.5, $p<0.05$ and CBZ vs wash diff in rank sum -3.5, ns). This effect might be due to the analysis.

Finally, carbamazepine does not significantly reduce the intensity of the SLE measured by the transmittance of the IOS signal (Friedman test in lesioned FS = 2.80, $p = 0.367$; sham FS = 5.43, $p = 0.085$; and contralateral FS = 1.75, $p = 0.531$).

Similarly, the application of lacosamide significantly increases the inter-event interval in lesioned slices and in sham alike. In most recordings there was a complete block of SLEs (Friedman test in **lesioned** FS = 13.56, $p<0.001$ and Dunn's multiple comparison test: baseline vs LCM diff. in rank sum -13.0, $p<0.01$ and LCM vs wash diff. in rank sum 14.0, $p<0.01$; in **sham** FS = 7.00, $p<0.05$ and Dunn's Multiple Comparison test: bas vs LCM d.i.r.s. -9.00, $p<0,05$, and LCM vs wash d.i.r.s. 6.00, ns). The increase in inter-event interval was not significant in contralateral slices (**contralateral** FS = 1.87, $p=0.355$).

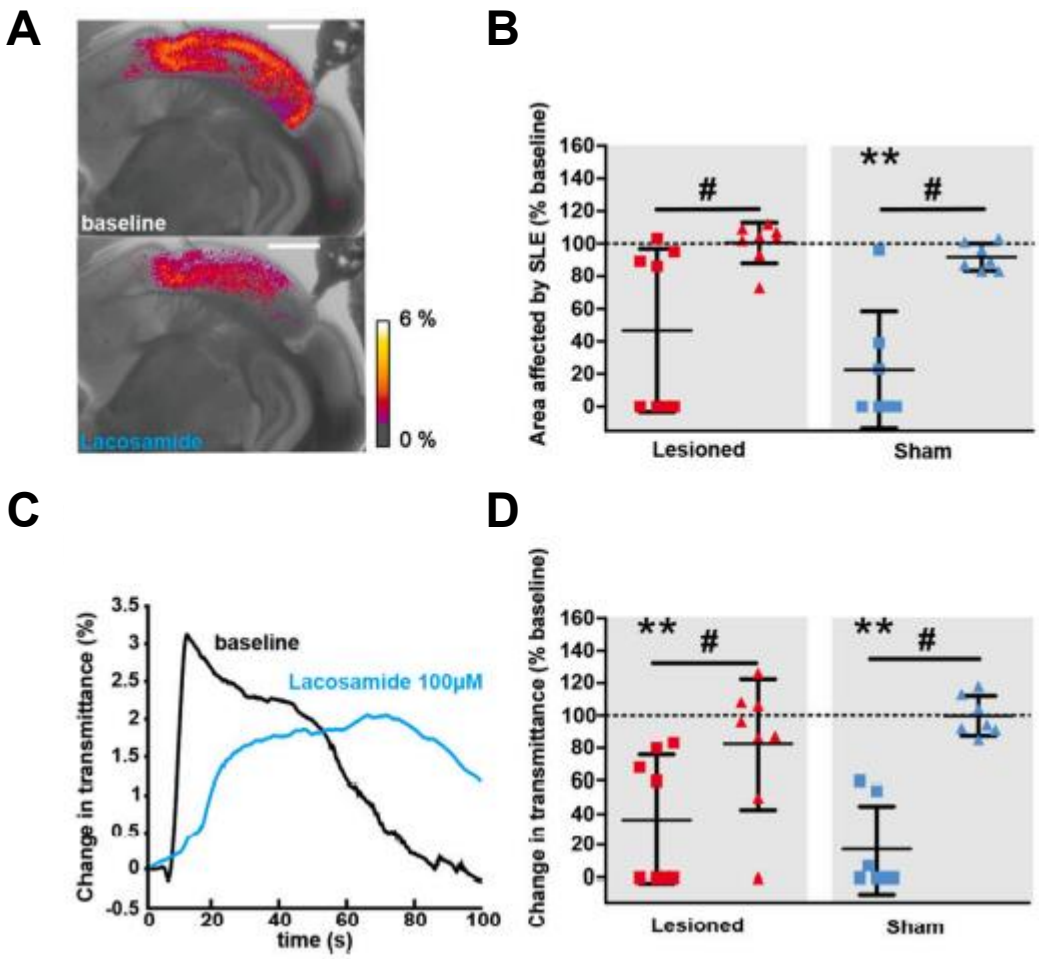

Figure 4 The sodium channel blocker lacosamide blocks the SLE by reducing the propagation of the SLE in the neocortex. A, B Lacosamide reduces drastically the area of the slice affected by the SLE (lesioned drug: 36.4 ± 39.5%, lesioned wash: 82.4 ± 40.0%, sham drug: 17.3 ± 27.3%, sham wash: 99.6 ± 12.3%). A. Representative images without and with lacosamide: IOS is color-coded; and B summary for all recordings. Scale bar: 1 mm. (C, D Lacosamide significantly reduces the maximum intensity of the IOS (lesioned drug: 46.6 ± 50.1%, lesioned wash: 100.4 ± 12.4%, sham drug: 22.6 ± 35.8%, sham wash: 91.7 ± 8.3. Representative time courses in the absence and presence of the drug and summary of effects for all groups. * Differences to baseline, # differences between drug application and washout (modified from Ragot et al., 2021).

Moreover, lacosamide diminishes the size of the area of the neocortex affected by the SLE (Friedman test in **lesioned** FS = 10.7, $p < 0.01$ and Dunn's multiple comparison test: bas. vs LCM diff. in rank sum 8.0, ns, and LCM vs wash d.i.r.s. -13.0, $p<0.01$; **sham** FS = 11.1, $p < 0,01$ and Dunn's multiple comparison test: baseline vs drug d.i.r.s. 12.0, $p<0,01$, and bas. vs wash d.i.r.s. -9.0, $p<0.05$; and **contralateral** FS = 9.38, $p < 0.01$ and Dunn's multiple comparison test: bas. vs drug d.i.r.s. 13.50, $p<0.01$, and baseline vs wash d.i.r.s. 7.5, ns), see Figure 4 A and B.

Lastly, lacosamide also weakens the change of transmittance during SLE in the lesioned slices as well as in the sham but the reduction is not significant in the contralateral slices

(Friedman test in **lesioned** FS = 9.75, $p < 0.01$ and Dunn's multiple comparison test: bas. vs LCM d.i.r.s. 12.0, $p<0.01$ and LCM vs wash: d.i.r.s. -9.0, $p<0.05$; **sham** FS = 10.6, $p < 0.01$ and Dunn's multiple comparison test: baseline vs LCM d.i.r.s. 11.0, $p<0.01$ and LCM vs wash: d.i.r.s. -10.0, $p<0.05$; and **contralateral** FS = 5.59, $p = 0.066$), see Figure 4 C and D.

3.7 Acetazolamide and zonisamide have antiepileptic effects, independent of the lesion.

Contrarily to the sodium channel blockers, acetazolamide (ATZ) and zonisamide (ZNS) scale down the epileptiform activity but do not fully stop the events. Acetazolamide is a carbonic anhydrase inhibitor and zonisamide has many targets: voltage-sensitive sodium and T-type calcium channels and it can inhibit the carbonic anhydrase but weakly.

Acetazolamide increases the inter-event interval in the SmS in all groups without achieving a complete blockade of the events. (Friedman test comparison between baseline, drug and wash: in **lesioned** FS = 12.97, $p < 0.001$ and Dunn's Multiple Comparison test : baseline vs ATZ d.i.r.s. -13.5, $p<0.01$ and ATZ vs wash d.i.r.s. -10.5, $p<0.05$; **sham** FS = 8.67, $p < 0.01$ and Dunn's multiple comparison test : baseline vs drug d.i.r.s. -10.5 , $p<0.05$; baseline vs wash d.i.r.s. -7.50, ns ; and **contralateral** FS = 13.0, $p < 0.001$ and Dunn's multiple comparison test : baseline vs ATZ d.i.r.s. -14.0, $p<0.001$; baseline vs wash d.i.r.s -10.0, $p<0.05$).

Acetazolamide decreases the size of the area affected by the SLE only in the lesioned slices (Friedman test: in **lesioned** FS = 7.54, $p < 0.05$ and Dunn's multiple comparison test: baseline vs ATZ d.i.r.s. 12.0, $p<0.05$; ATZ vs wash -7.50, ns; **sham** FS = 2.70, $p = 0.252$; **contralateral** FS = 0.171, $p = 0.971$). However, acetazolamide has no significant effect on the intensity of the SLE in any of the groups (Friedman test in **lesioned** FS = 3.44, $p = 0.187$; **sham** FS = 0.783, $p = 0.740$; **contralateral** FS = 0.060, $p = 0.971$).

Zonisamide increases greatly the inter-event interval in the SmS both in the lesioned slices and the slices from the contralateral hemisphere but does not have a significant effect on the sham. (Friedman test comparison between baseline, drug, and wash: in **lesioned** FS = 10.3, $p < 0.01$ and Dunn's multiple comparison test: baseline vs ZNS d.i.r.s. -12.0, $p<0.01$ and ZNS vs wash d.i.r.s. 6.00, ns; **sham** FS = 2.89, $p = 0.278$; and **contralateral** FS = 7.14, $p < 0.05$ and Dunn's multiple comparison test: baseline vs ZNS

d.i.r.s. -10.00, p<0.05; ZNS vs wash d.i.r.s 5.00, ns). This might indicate that the contralateral hemisphere in the lesioned animals is also altered by the freeze-lesion.

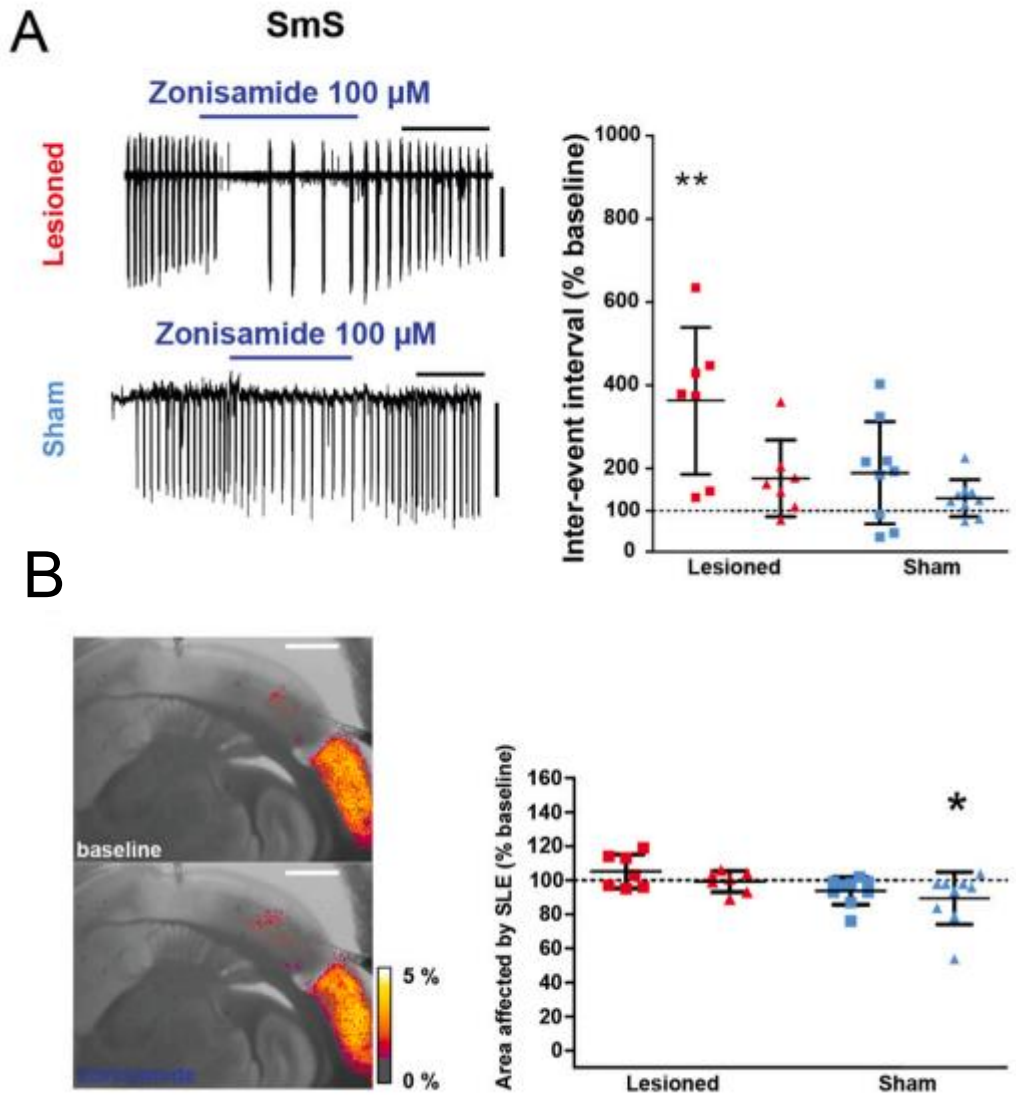

Figure 5 Zonisamide's mode of action is not linked to a reduction of the propagation of SLE. A. Representative traces and graph of all individual recordings, zonisamide reduced SLE frequency in the lesioned slices A (lesioned drug: 363.4 ± 176.0%, lesioned wash: 177.2 ± 91.3%, sham drug: 190.4 ± 122.2%, sham wash: 130.1 ± 44.2) in the SmS. Blue lines indicate time interval of drug application. Scale bars: 2 mV, 30 min. B. Zonisamide (lesioned drug: 105.3 ± 9.9%, lesioned wash: 99.3 ± 6.2%, sham drug: 93.8 ± 8.0%, sham wash: 89.4 ± 15.4%) has no impact on the size of the area affected by the SLE. Representative images in absence and presence of zonisamide (left): IOS is color-coded; and graph of all recordings (right). Scale bar: 1 mm (modified from Ragot et al., 2021).

Zonisamide has no effect on the size of the area affected by the SLE in any of the groups. (Friedman test in **lesioned** FS = 0.518, p= 0.768; **sham** FS = 8.63, p < 0.05 and Dunn's multiple comparison test: baseline vs ZNS d.i.r.s. 9.5, ns and bas. vs wash d.i.r.s. 11.5, p<0.05; and **contralateral** FS = 0.5806, p =0.7943). The difference observed in the sham is only due to a decrease in the SLE area during wash (after 2h of recordings) and therefore could be a sign of a fatigue/loss of energy in some of the slices. Furthermore, the intensity of the SLEs measured as the maximum change in transmittance in the slice does not change upon wash in of zonisamide in any of the groups (Friedman test in **lesioned** FS = 1.14, p= 0.620; **sham** FS = 1.56, p= 0.569; and **contralateral** FS = 2.47, p = 0.285), see Figure 5

4. Discussion

4.1 Reproducibility and relevance of the focal freeze lesion model

As described in the Results section, the FFLM produced a highly consistent microgyrus-like lesion with a very low mortality rate in the pups (50). The FFLM reproduces some mechanisms and macroscopic lesions seen in MCD, especially microgyria (60) or schizencephaly (59). The protocol used led to the formation of only one microgyrus, however its perisylvian location recreates the most frequent pattern of polymicrogyria: 61% in a cohort of 328 patients (10), and 77% in a cohort of 87 patients (61).

The use of male pups hinged mainly on the need to exclude the potential influence of menstrual cycle hormones on the results. This decision can be further clinically justified, because in polymicrogyria, the majority of the patients are male (10).

4.2 MRI scans showed a reduction in hemisphere volume in the lesioned animals

The lesioned hemispheres were significantly smaller than the contralateral, with volume difference up to 10%, according to MRI measures. A "tissue reduction" had been observed previously in this model (58) but this is the first time this volume difference is quantitatively assessed (50).

The loss of volume was mostly limited to neocortical areas (no difference existed between hippocampi). More precise measurements were, however, not possible due to the high-speed acquisition protocol with a scan width of 0.75 mm, precluding delineation of the lesion precise enough to estimate volume changes in smaller structures.

As the microgyrus makes up less than 1% of the hemisphere volume, such significant reduction in brain volume in the lesioned hemisphere cannot be attributed to the formation of the microgyrus alone and may be related to the previously reported widespread loss of thalamocortical afferents and thalamic nuclei (26,28,62).

This result is in line with what can be seen in patients. Microcephaly is a common comorbidity in patients with polymicrogyria: a study found microcephaly in 50% of the cohort of 118 patients (10) .

4.3 Absence of spontaneous seizures in the neonatal focal freeze lesion model

Despite the similarities with MCDs, one important limit of the neonatal FFLM is the absence of spontaneous seizures in the animals, contrary to the in-utero freeze lesion. Kamada and colleagues were notably able to record long lasting seizures in the EEG of FFL rats, after bilaterally freeze-lesioning rat embryos (at E18) from outside the uterus wall (63).

Seizures in the neonatal FFLM can only be observed after a “second hit”. They must be either evoked by stimulation (25,26,58,64,65), provoked in vivo, e.g. by kainic acid injection (27), hypothermia (30) or hyperthermia (Awad et al., 2016), or induced in slices by bath application of solutions capable of lowering the seizure threshold like low-Mg^{2+} aCSF (32) or 4-aminopyridine (50).

4.4 Induction of seizure-like events with 4-aminopyridine

The non-specific K+ channel blocker 4AP was chosen for its ability to induce SLE activity in rat neocortical slices lasting several hours, it is robust enough to produce identifiable IOS (56).

The bath application of 4AP produced similar SLE in lesioned and sham animals (50) confirming that 4AP is sufficient to induce such ictal activity (57). Contrarily to what was expected, the SLEs occurred as frequently in the lesioned slices as in the controls, they also presented the same parameters and propagated in the slice along the same pathways (50). Considering that 4AP may alter the chloride homeostasis (67,68), employing a different type of “second hit” to generate SLE could have confirmed lesion-specific AED effects and strengthened the translational significance of our findings.

The long lasting SLEs induced by 4AP are associated with an increase in $[K+]_e$ (69), following the activation of $GABA_A$ receptors. Paradoxically, this increase of $[K+]_e$, could if the epileptic state is maintained shift E_{GABA} and weaken the inhibition. This hypothesis can explain long term effect of epilepsy in patients. It is, however very unlikely to happen in our model where the whole experiment from beginning of induction of the seizures to end of phase 3 lasts 3h.

4.5 IOS analysis confirms the onset site of SLE is in the perilesional area

The perilesional area (or paramicrogyral zone, PMZ) is known to be hyperexcitable in the FFLM, due to an abnormal innervation of the area by cortical and subcortical excitatory afferents (25). I examined whether the perilesional area would produce SLE "spontaneously" in a context of lowered threshold. In the lesioned slices, the onset site was indeed in majority of cases in the perilesional area, whereas the points of origin of the SLE were more spread out in the control groups (50).

More precisely, the onset of SLE in the lesioned slices was on average at a distance of 1.8 mm from the center of the microgyrus, and SLE always started in layers II/III (50). It is interesting to note that "dense patches of thalamocortical terminations" have been observed in these exact layers and location (28) and are thought to be one of the bases of the hyperexcitability of the perilesional area.

As expected, I did not record any SLE starting in the microgyrus, however, some SLE sometimes propagated to or through the microgyrus. The propagation of the event through the microgyrus was always faster in the upper layers (50) which are composed of neurons born on E17,5 that invaded the microgyrus after the necrosis and are in majority glutamatergic [at least at P4] (47).

4.6 In other models of MCD, the malformation remains interconnected with the neighbouring hyperexcitable normo-typic cortex

In a targeted genetic model [Dcx- KD rats] of subcortical band heterotopia (SBH or double cortex syndrome), the normo-typic cortex had a major role in the induction of interictal events and seizures. Interestingly, the inter-ictal like events induced by bicuculine (blockade of $GABA_A$ receptors), did not start in the ectopic neurons of the subcortical band but were initiated in the normo-typic cortex directly above it (70). Similarly, to our results

in the FFLM, where the SLE sometimes propagated through the microgyrus (50), these events propagated to the ectopic neurons that seemed to be integrated to the cortical circuitry.

MRI studies on patients with a different MCD (cortical heterotopia) show abnormal neuronal activation initiated within or adjacent to the heterotopia, involving the overlying normo-typic cortex (71–73). Interneurons were found inside the heterotopia in normal numbers, but they were “randomly oriented with little apparent organization”(74). All this suggests that the ectopic cells remain interconnected with the normo-typic cortex.

4.7 Non-lesion specific effects of the AEDs on our model of MCD

The mode of action of AEDs can be based on two main mechanisms: they can prevent the onset of SLE by elevating the seizure threshold or they can impair the propagation of the SLE. The AEDs tested have different targets and suspected mode of actions. By analysing the IOS, their impact on the propagation of the SLE was calculated (50), which brings new information on the mode of actions of these AEDs.

4.7.1 Carbamazepine

Carbamazepine is a widely used AED believed to act mainly on voltage-gated sodium channels via binding to their inactivated state. Studies indicate that this inactivation of the sodium channels leads to a decrease of excitability which elevates the threshold for seizures in kindling models of epilepsy (17,75). Carbamazepine is used clinically to prevent focal as well as tonic-clonic seizures.

As previously described, carbamazepine blocked efficiently 4AP-induced SLEs in the sham (57). Carbamazepine also blocked SLE in the lesioned slices and in the contralateral slices (50). The effect of carbamazepine was therefore not lesion-specific.

Carbamazepine’s mode of action and the fact that it decreases gamma power signal (50-60Hz) – an indicator of the abnormal synchronization of local cortical activity, therefore a marker of the start of an epileptic seizure - suggests an action on the onset of seizure (76).

However, carbamazepine seems to also have a role in limiting the propagation of seizures through its binding to Nav1.1, a voltage-gated sodium channel essential for action propagation (specifically, to the a1 subunit encoded by SCN1A). Indeed, the pre-

operative withdrawal of carbamazepine increased the duration (and propagation) of the seizures but did not modify the ictal EEG localization (77).

In conclusion, there are arguments in the literature in favour of the two modes of action: disturbing seizure initiation and reducing the propagation, although the main antiepileptic effect of carbamazepine is thought on seizure initiation (17,78).

Interestingly, I showed that the size of the area of propagation was reduced only in the lesioned slices (50), before all ictal activity was inhibited in these slices too. The delayed block of all SLE in the lesioned slices compared to controls could be an effect of the hyperexcitability in the perilesional area.

However, the differential effect in size of the area of propagation between lesioned and controls was biased by the wash in-dynamics. All SLE occurring during the wash in period were included to measure the mean area affected by the SLE. Since SLE were blocked by carbamazepine in most slices, the number of SLE included in this calculation was quite low. Moreover, the faster the epileptiform activity was hindered by carbamazepine, the lower the number of SLE analysed. Consequently, the difference between lesioned slices and the controls could be an artefact of the analysis and not a lesion specific pharmacological effect.

Overall, these results do not permit to identify a single mode of action of carbamazepine but rather confirm a dual effect of this AED. The complete block of SLE suggests an antiepileptic effect based on elevation of the seizure threshold and a reduction of the neuronal excitability at the onset site. But the significant reduction in the size of the SLE area in the lesioned slices points to an impact on the propagation of the SLE.

4.7.2 Lacosamide

The functionalized amino acid, lacosamide, belongs to the new generation of sodium channel blockers approved for clinical use in the EU in 2008. It is effective in patients with intractable epilepsy and is often used as an adjunctive treatment (three trials of over 1200 patients demonstrated its effectiveness and safety: (79–81). According to a recent meta-analysis (82), lacosamide is “generally effective and well tolerated to use in children with epilepsy".

Lacosamide decreased both inter-ictal spikes and high frequency oscillations (HFOs) in the pilocarpine model of mesial temporal lobe epilepsy (MTLE) (83). In a kindling model, lacosamide appeared to reduce seizure initiation (17).

In vitro, lacosamide suppresses epileptiform activity induced by 4AP in the brain slices (56,84). I confirmed this effect, as lacosamide (like carbamazepine) fully blocked SLE in both controls and in the lesioned slices (50). Lacosamide also diminishes the size of the area affected by the SLE and diminishes the strength of the IOS. In our model, lacosamide has therefore a clear impact on seizure propagation, even though this effect is not lesion-specific (50). This mode of action can be explained by its suspected targets.

While the majority of the first generations of AEDs (such as carbamazepine) act on voltage-gated sodium channels (Na_v), by stabilizing their fast inactivation, lacosamide promotes Na_v slow inactivation (which is crucial for the regulation of neuronal firing properties) (85). As indicated by their name, Na_v recover faster from “fast inactivation” (<100 ms) than from the “slow inactivation” (around 5-10 s) (86). Lacosamide therefore maintains Na_v in an inactivated state which would reduce the propagation of seizures. Finally, lacosamide was found to have an effect on A-type K+current IK(A), which was concentration-dependent and elicited a response to membrane depolarization (87).

4.7.3 Zonisamide

Zonisamide is a broad-spectrum sulfonamide compound developed in Japan: it is used for the treatment of focal and generalised seizures, since its entry on the market in 2005.

I showed that zonisamide, contrarily to the sodium channel blockers, reduced the frequency of SLE without fully blocking the ictal activity in the lesioned and contralateral slices but not in the sham (50). The discrepancy between the two controls, makes the interpretation of this result difficult (I will discuss the interpretation of results from the “contralateral group” in more details later).

Several elements point towards a non-lesion-specific effect of zonisamide. Firstly, recordings in the second field potential electrode (in the Ect cortex) show a reduction of the SLE frequency similar in all three groups. Moreover, the location of the onset of

seizure was not modified by zonisamide (contrarily to the effect of bumetanide)(50). On the other end, the mode of action of zonisamide in this experiment was very clear: in all three groups, the area of propagation was not reduced by zonisamide, neither was the intensity of the IOS. In general, the characteristics of the SLE remained unmodified by zonisamide and only their frequency diminished (50). This mode of action is unexpected and might be related to the use of 4AP to induce SLE.

Zonisamide is a T-type calcium channel blocker (88) and influences voltage-dependent sodium channels as well, leading to a suppression of repetitive firing. Zonisamide is also a carbonic anhydrase inhibitor, but this does not seem to have a strong antiepileptic impact since high concentrations of the AED are required to see any effect on the carbonic anhydrase (89–91).

In an in vivo model of generalised seizures, induced by cortical freezing in cats, zonisamide stopped the cortical spiking from developing into full generalised seizures (90). Similar blockade of the propagation of seizures was observed in a kindling model in cats (92). The secondary propagation from limbic structures into the thamalus and the SmS cortex of kainic acid induced SLE was attenuated by zonisamide in freely moving rats. (93). Taken together, these results suggest that zonisamide's mode of action is to primarily to limit the propagation of seizures.

4.7.4 Acetazolamide

Acetazolamide is a carbonic anhydrase blocker discovered in 1940 (94), it is 100-1000 times more potent than zonisamide (91). A recent meta-analysis of clinical studies in focal and generalised epilepsy found that acetazolamide at least halved the number of seizures in 48% of participants (the responder rate varied from 23% to 79%), and the average seizure freedom rate was impressively 20% (varying between 6% and 63%) (95).

Acetazolamide reduced the frequency of the SLE in all three groups in our model (50) by preventing the initiation of long ictal events similarly to previous studies (96), yet the effect was more significant in the lesioned slices. Interestingly, acetazolamide also limited the propagation of the SLE in the lesioned slice specifically (50), revealing a different mode of action. This complex effect in the model could be due to the fact that this AED has several mechanisms of action, activating various molecular pathways simultaneously.

In a study in vitro, acetazolamide decreased both the duration and the frequency of SLE, induced by 4AP in the neocortex, without affecting their frequency (96). The authors showed that removing intracellular HCO_3^- or inhibiting $GABA_A$ receptors completely stopped the 4AP-induced SLE and concluded that acetazolamide reversed GABA current from depolarising to hyperpolarising in this experiment, the depolarising GABA being caused by the application of 4AP (96). E_{GABA} was however not measured per se in this study.

On the other hand, acetazolamide blocked 4AP-induced SLE in the hippocampus of neonatal rats only at a specific age. Indeed acetazolamide, blocked 80-100% of the SLE only between P6-P19 (55), the period during which GABA is depolarising.

In the hypothesis that an immature network persists in adulthood in the FFLM, acetazolamide could therefore also be specifically effective in the lesioned slices.

The carbonic anhydrase (CA) is an enzyme catalysing the following reaction:

$CO_2 + H_2O \rightarrow HCO_3^- + H^+$

The inhibition of this enzyme can increase the seizure threshold via effects of its two products: by generating intracellular acidosis and by lowering the level of intracellular bicarbonate. The difference of acidification (reduction of pH by 0.2) between the areas of a slice involved in the ictal activity or not demonstrated the importance of slight variations of pH in epileptogenicity (97). Indeed, protons at the cell membrane can interact with receptors such as NMDA receptors, $GABA_A$ and glycine receptors and modulate their activity (95,98).

On the other hand, the intracellular concentration of bicarbonate, actively maintained by CA, could render $GABA_A$ depolarising, in situations where the chloride driving force is weakened (for example after a period of maintained epileptic activity). In this context, acetazolamide would help switch $GABA_A$ back to a hyperpolarising action.

Another pathway is also activated by the carbonic anhydrase: via the acid sensing ion channels (ASIC), present in astrocytes, which are voltage-dependent proton-gated cation channels. They sense acidity in the extracellular environment, and at certain ranges of pH, release Na^+ and Ca^{2+} into the cell (82). They can therefore cause a small depolarisation, sufficient to activate NMDA receptors, $GABA_A$ and glycine receptors. ASIC1 are expressed in activated astrocytes, in the sclerotic hippocampus of epileptic

mice and patients with temporal lobe epilepsy, and these channels participated in the pilocarpine-induced epileptogenesis (99).

The mode of action of carbonic anhydrase blocker, such as acetazolamide is therefore complex, and the relative impact of each pathway is not fully understood.

4.8 Lesion specific effect of the NKCC1 blocker bumetanide in adult FFLM

$GABA_A$ receptors are permeable to chloride and carbonate ions (on a smaller scale). In the adult brain, the activation of $GABA_A$ usually creates a hyperpolarising current due to the chloride gradient, mostly maintained by chloride cotransporters: NKCC1 and KCC2.

Bumetanide is an established diuretic via its inhibition of both chloride cotransporters. At a low concentration though, bumetanide is a specific inhibitor of NKCC1 (100). In epilepsy, the consequences of the inhibition of NKCC1, which is a marker of an immature network in the brain and whose expression is usually associated with abnormally depolarising GABA in adults, has been thoroughly investigated in animal models.

In the rat, the neonatal brain is at a stage of development corresponding to the last trimester of human pregnancy. Therefore, at birth GABA is still depolarising and the migration of neurons from the cortical subplate is on-going. In fact, in the neonatal neocortex in the rat, KCC2 is expressed at only 5-15% of the level of adult brain while NKCC1 is highly expressed until postnatal day 14 (42). The shift to hyperpolarising GABA is progressive and completed in the rat neocortex at P15.

In vitro, bumetanide was shown to be effective in neonatal cortical slices (P6-P9) to stop 4AP-induced interictal seizures and to prevent the apparition of ictal events (101). In another study, bumetanide suppressed 4AP-induced SLE in the CA3 but not in the Ect cortex at P4 but not P7 (55).

On the other hand, in a model of febrile seizures combining freeze lesioning at P1 and hyperthermia at P10 showed an over-expression of KCC2 in the ipsilateral hippocampus at P20. Constantly, with these results, E_{GABA} was hyperpolarising in this model (66). The double hit in this model, which would induce high excitability in the hippocampus and neocortex, probably triggered the overexpression of KCC2 as a compensatory mechanism.

Several studies showed an effect of bumetanide in adult network, indicating the persistence of an immature network in models of epilepsy. Bumetanide reduced pilocarpine-induced SLE (102); it also decreased kainic acid-induced SLE in vivo and 0Mg-induced SLE in vitro (103). Alternatively, bumetanide (at a dose specific to NKCC1) failed to reduce SLE, induced by 4AP, while specific KCC2 blockers blocked the ictal activity, replacing the long SLE by continuous interictal events (104).

Finally, in the FFLM, NKCC1 is overexpressed during the formation of the microgyrus, in the perilesional area (Shimizu-Okabe, Tanaka and Matsuda, 2011), but returns to expected expression levels after two weeks. Additionally, bumetanide has been shown to have an effect in the first weeks after the freeze lesion (47), but this effect decreased over time, and bumetanide had no effect in adult slices.

As far as I know, I showed for the first time an effect of bumetanide in the adult freeze-lesioned rat (50). Bumetanide significantly reduced the frequency of SLE in the perilesional area specifically and shifted the onset site away from the lesion, (50), confirming that bumetanide has a molecular target in the perilesional area. This concurs with the hypothesis that consequently to the freeze lesion, the perilesional area is maintained in an immature state, with the persistence of NKCC1 cotransporter in adulthood.

Our results corroborate previous findings of altered GABA function in MCD and imply the modulation of the Cl- homeostasis as a promising target for antiepileptic treatment in this disease spectrum.

4.8.1 Concept of neuroarcheology

In 2008, Professor Ben Ari coined the concept of neuroarcheology, which is defined as a study of early signs of neurological diseases during the development of the brain, encompassing not only mutations leading to aberrant proteins but also environmental and genetic events leading to an alteration of the precise plan of neurodevelopment (105). Prof Ben Ari concludes that “misplaced neurons disturb preferentially during development an ensemble of structures they were programmed to operate with”.

In this dissertation, I precisely interrogate this hypothesis, in the context of a visible malformation of the cortex similar to what can be seen in patients with microgyria.

By measuring the propagation of seizure-like event occurring spontaneously, in a context where the level of excitability of the brain had been increased, I demonstrated a distant effect of a focal lesion. Moreover, by measuring this seizure-like activity in young adult brains after the lesion was created in the new-born animals, I present long-term effect of a disorganisation of the cortical architecture. I showed that the electrical activity in the lesioned slices can be compared to that of an immature brain, further corroborating the hypothesis of a “frozen immature structure” (36).

4.8.2 The effect of bumetanide shown in our study might not be due to the persistence of NKCC1 in cortical neurons.

I did not show the presence of NKCC1 per se in the freeze-lesioned slices (50). Even though bumetanide has been shown to be specific to NKCC1 at the concentration used (10µM) (100), the measure of the mRNA and protein expression of both KCC2 and NKCC1 would have increased the robustness of our results.

Recent investigations of the mechanisms of action of bumetanide suggest that its effect notably in patient could be the consequence of inhibition of NKCC1 expressed in glial cells. Further immuno-histological studies of this model would be interesting to see if the targets of bumetanide are located in neurons or also in glial cells.

4.8.3 Bumetanide does not pass the blood brain barrier

The use of bumetanide in treatment of neurological disorders is still controversial as it was shown early on that it might poorly penetrate the blood-brain barrier or BBB (106).

The efficacy of bumetanide to block seizures in neonatal rats (42,55,101) and its proven safety as an approved antidiuretic have, however, led to clinical trials in young children. The protective role of bumetanide in neonatal seizure activity in human neonates was shown on isolated cases (107). A large-scale phase 1 and 2 trial (NEMO Trial) was conducted to evaluate the effect of bumetanide as an add-on to phenobarbital, in the treatment of neonatal seizures. This trial was however stopped early, due high rate (27% of the cohort) of hearing loss in the children (108). Nevertheless, a recent study in 27 neonates indicated low-side effects (even though 8% of the children had hearing impairment) and an interesting impact on children mortality in neonatal seizures (109).

Further studies have since then questioned whether a sufficient dose of bumetanide to activate central targets passes the BBB and is able to enter the brain (110,111). Because

bumetanide binds to plasma protein very efficiently, and has difficulties crossing the BBB, only about 0.3% of the total plasma concentration is available as unbound concentration in the brain (112). The concentration of bumetanide in the brain, appears to be too low to block NKCC1 (113).

This question, associated with the failure of the NEMO trial, have fuelled a debate on the exact molecular targets of bumetanide in vivo and whether the effects of bumetanide in children with epilepsy and in patients with autistic syndrome could be due a peripheral effect (114–117).

A few alternative molecules have been developed, close in structure to bumetanide, that penetrate more efficiently the brain. Bumepamine is candidate successor to bumetanide and has potential as an adjuvant to phenobarbital, however, it does not block NKCC1 (118). The prodrug BUM5 was able to potentiate the effect of phenobarbital in adult epileptic mice when bumetanide did not.(119). Recently, azosemide was proposed as an alternative NKCC1 inhibitor (120).

In the context of MCD, the blood-brain barrier might also be partially damaged, and its permeability could be different than what was measured in healthy animals. Indeed, polymicrogyria has been linked with tight junction and BBB dysfunction (121).

4.9 The complicated case of the contralateral hemisphere

The protocol for our study (50) included the use of two controls: the contralateral hemisphere from lesioned animals and sham animals. I therefore induced and recorded SLE in slices from the lesioned hemisphere and in both controls identically. However, during the analysis of the results it appeared apparent that the contralateral hemisphere was not a perfect control. Depending on the AED tested, the effect on the contralateral slices was either similar to the effect in the sham (bumetanide, carbamazepine and acetazolamide), similar to the lesioned slices (zonisamide) or was unique to the contralateral slices (lacosamide).

To be more precise, similarly to its effect on sham slices, bumetanide had no impact on the frequency of SLE or the IOS parameters in contralateral slices. Both carbamazepine and acetazolamide effectively inhibited SLE in the contralateral slices with the same efficiency as in the sham, but they had no effect on the IOS parameters.

Contrarily, lacosamide reduced the frequency of SLE in both lesioned and sham slices while having no influence on the frequency in contralateral slices. Additionally, lacosamide actively diminished the propagation of SLE in the contralateral slices, in a manner similar to lesioned and sham animals.

Lastly, zonisamide decreased the frequency of SLE both in lesioned slices and in contralateral slices but not in the sham. This confirms that the effect of zonisamide on SLE is not lesion-specific.

As the complexity of the effects of the AEDs on the contralateral hemispheres diminished the readability of our results, we decided to present the results of this group in a separate figure for their publication (50). However, all results for the contralateral group and statistical data are presented in the Results section, in comparison with the lesioned and sham groups.

The variable effects of AEDs on the contralateral slices question a possible involvement in the pathomechanism of MCD in regions far from the lesion, even in the contralateral hemisphere, via callosal connections. Studies have shown that one hemisphere can recruit the other to increase its processing capacity, in case of a deficiency, or a lesion in the dominant hemisphere (122,123), notably in perinatal brain injuries (124). In the FFLM, widespread changes in connectivity have been reported, notably modified callosal, thalamocortical, and cortico-thalamic connections (28).

It is possible to hypothesize that after the freeze lesioning, afferents from the contralateral hemisphere could be recruited thus creating abnormal interhemispheric connectivity between the perilesional area and the contralateral hemisphere.

In the FFLM, the contralateral hemisphere should therefore be considered as a limited control for the lesioned hemisphere, with a physiology in an intermediary position between diseased and healthy.

4.10 Opening – new perspectives in treatment of epilepsy outside of AEDs

In this dissertation, I've explained the necessity to get a better understanding of the mode of action of AEDs which may allow for lesion- or etiology-specific ("personalized") choice

of AEDs. Moreover, I presented the surgical removal of the epileptogenic area as the best treatment option in well-selected patients with drug-resistant epilepsy.

It is worth mentioning that the surgical techniques have improved greatly in the last years, with the introduction of technology in the operating room, helping to limit the risk of complications and to improve the chance of seizure freedom post-surgery. Better imaging tools (based on MRI) help define with high precision the epileptogenic area, which makes resection surgeries mostly successful in patients with intractable epilepsy (14) though the results are not as good in case of MCD (125)

Nevertheless, resective surgeries remain invasive and are not always possible depending on location of the epileptogenic area. Finally, they can have long term negative effects even when the surgery goes according to plan. In fact, serious long-term effects on patient personality which has been shown recently (126) .

Alternative approaches are also being developed such as deep brain stimulation. Indeed, recently a closed-loop stimulation of GABAergic cells in the medial septum, which project into the hippocampus and entorhinal cortex, was shown to reduce significantly the seizures in rodent models of temporal lobe epilepsy ((127,128)

Translating basic science to treatments is very challenging. Indeed, over 90% of drugs coming out of preclinical research fail during the clinical phase and do not get approval from the regulatory agencies (129,130). On top of that, the cost of producing new drugs increases every year for the pharmaceutical industries (130).

In this context, getting a better understanding of the mechanisms of action of already approved drugs and refining their use by targeting specific subgroups of patients, may be the fastest and best way to offer treatment to patients with rare types of epilepsies.

Bibliography

1. World Health Organisation. EPILEPSY A public health imperative International League Against Epilepsy [Internet]. 2019. Available from: https://www.who.int/about/licensing.
2. Fiest KM, Sauro KM, Wiebe S, Patten SB, Dykeman J, Pringsheim T, et al. Prevalence and incidence of Epilepsy - A systematic review and meta-analysis of international studies. Neurology. 2017;
3. Hirtz D, Thurman DJ, Gwinn-Hardy K, Mohamed M, Chaudhuri a R, Zalutsky R. How common are the 'common' neurologic disorders? Neurology [Internet]. 2007 Jan 30;68(5):326–37. Available from: http://www.ncbi.nlm.nih.gov/pubmed/17261678
4. Takano T, Sokoda T, Akahori S, Sakaue Y, Sawai C, Takeuchi Y, et al. Enhanced Capacity of Epilepsy in Brain Malformation Produced During Early Development. Pediatr Neurol. 2006 Jul;35(1):38–41.
5. Şah O, Türkdoğan D, Küçük S, Takış G, Asadov R, Öztürk G, et al. Neurodevelopmental findings and epilepsy in malformations of cortical development. Turkish Archives of Pediatrics. 2021;56(4):356–65.
6. Venti V, Consentino MC, Smilari P, Greco F, Oliva CF, Fiumara A, et al. Malformations of cortical development, cognitive involvement and epilepsy: A single institution experience in 19 young patients. Children. 2021 Aug 1;8(8).
7. Chen W, Jin B, Aung T, He C, Chen C, Wang S, et al. Response to antiseizure medications in epileptic patients with malformation of cortical development. Ther Adv Neurol Disord. 2021;14.
8. Guerrini R, Dobyns W. Malformations of cortical development: clinical features and genetic causes. Lancet Neurology. 2014;176(1):139–48.
9. Klingler E, Francis F, Jabaudon D, Cappello S. Mapping the molecular and cellular complexity of cortical malformations. Science (1979) [Internet]. 2021 Jan 22;371(6527):4517. Available from: https://www.science.org/doi/10.1126/science.aba4517
10. Leventer RJ, Jansen A, Pilz DT, Stoodley N, Marini C, Dubeau F, et al. Clinical and imaging heterogeneity of polymicrogyria: A study of 328 patients. Brain. 2010 May;133(5):1415–27.
11. Kwan P, Arzimanoglou A, Berg AT, Brodie MJ, Hauser WA, Mathern G, et al. Definition of drug resistant epilepsy: Consensus proposal by the ad hoc Task Force of the ILAE Commission on Therapeutic Strategies. Epilepsia. 2010;51(6):1069–77.
12. Chen Z, Brodie MJ, Liew D, Kwan P. Treatment outcomes in patients with newly diagnosed epilepsy treated with established and new antiepileptic drugs a 30-year longitudinal cohort study. JAMA Neurol. 2018 Mar 1;75(3):279–86.
13. Kwan P, Arzimanoglou A, Berg AT, Brodie MJ, Hauser WA, Mathern G, et al. Definition of drug resistant epilepsy: Consensus proposal by the ad hoc Task Force of the ILAE Commission on Therapeutic Strategies. Vol. 51, Epilepsia. 2010. p. 1069–77.
14. Sheng J, Liu S, Qin H, Li B, Zhang X. Drug-Resistant Epilepsy and Surgery. Curr Neuropharmacol. 2017 Jun 30;16(1).

15. Kwon HE, Kim SH, Kang HC, Lee JS, Kim HD. Epilepsy surgery for pediatric patients with mild malformation of cortical development. Seizure. 2020 Nov 1;82:50–5.

16. Barba C, Cossu M, Guerrini R, di Gennaro G, Villani F, de Palma L, et al. Temporal lobe epilepsy surgery in children and adults: A multicenter study. Epilepsia. 2021 Jan 1;62(1):128–42.

17. Wu T, Ido K, Ohgoh M, Hanada T. Mode of seizure inhibition by sodium channel blockers, an SV2A ligand, and an AMPA receptor antagonist in a rat amygdala kindling model. Epilepsy Res. 2019 Aug 1;154:42–9.

18. Dvorak K FJ. Migration of neuroblasts through partial ne- crosis of the cerebral cortex in newborn rats. Contribution to the problems of morphological development and developmental period of cerebral microgyria. Acta Neuropathol. 1977;38:203–212.

19. Luhmann HL. Cortical malformations as a cause for epileptiform activity: The freeze lesion Model - Encyclopedia of Basic Epilepsy Research, vol.1, pp. 187-191. Encycloped. Vol. 1. 2009. 187–191 p.

20. Dvořàk K, Feit J, Juránková Z. Experimentally induced focal microgyria and status verrucosus deformis in rats — Pathogenesis and interrelation histological and autoradiographical study. Acta Neuropathol [Internet]. 1978 Jan;44(2):121–9. Available from: http://link.springer.com/10.1007/BF00691477

21. Rosen GD, Press DM, Sherman GF, Galaburda AM. The Development of Induced Cerebrocortical Microgyria in the Rat. J Neuropathol Exp Neurol [Internet]. 1992 Nov;51(6):601–11. Available from: https://academic.oup.com/jnen/article-lookup/doi/10.1097/00005072-199211000-00005

22. Jacobs KM, Hwang BJ, Prince DA. Focal epileptogenesis in a rat model of polymicrogyria. J Neurophysiol. 1999;81(1):159–73.

23. Raymond AA, Fish DR, Sisodiya SM, Alsanjari N, Stevens JM, Shorvon SD. Abnormalities of gyration, heterotopias, tuberous sclerosis, focal cortical dysplasia, microdysgenesis, dysembryoplastic neuroepithelial tumour and dysgenesis of the archicortex in epilepsy: Clinical, EEG and neuroimaging features in 100 adult patients. Brain [Internet]. 1995;118(3):629–60. Available from: https://academic.oup.com/brain/article-lookup/doi/10.1093/brain/118.3.629

24. Bartolomei F, Gavaret M, Dravet C, Guye M, Bally-Berard JY, Genton P, et al. Late-Onset Epilepsy Associated with Regional Brain Cortical Dysplasia. Vol. 42, Eur Neurol. 1999.

25. Jacobs KM, Gutnick MJ, Prince DA. Hyperexcitability in a Model of Cortical Maldevelopment. Cerebral Cortex [Internet]. 1996;6(3):514–23. Available from: https://academic.oup.com/cercor/article-lookup/doi/10.1093/cercor/6.3.514

26. Jacobs KM, Mogensen M, Warren E, Prince DA. Experimental Microgyri Disrupt the Barrel Field Pattern in Rat Somatosensory Cortex. Cerebral Cortex [Internet]. 1999 Oct 1;9(7):733–44. Available from: https://academic.oup.com/cercor/article-lookup/doi/10.1093/cercor/9.7.733

27. Andresen L, Hampton D, Taylor A, Morel L, Yang Y, Maguire J, et al. Gabapentin attenuates hyperexcitability in the freeze-lesion model of developmental cortical malformation. Neurobiol Dis. 2014;18(9):1199–216.

28. Rosen GD, Burstein D, Galaburda AM. Changes in efferent and afferent connectivity in rats with induced cerebrocortical microgyria. Journal of Comparative Neurology. 2000;418(4):423–40.

29. Redecker C, Luhmann HJ, Hagemann G, Fritschy J marc, Witte OW. Differential Downregulation of GABA A Receptor Subunits in Widespread Brain Regions in the Freeze-Lesion Model of Focal Cortical Malformations. The Journal of Neuroscience. 2000;20(13):5045–53.

30. Kellinghaus C, Möddel G, Shigeto H, Ying Z, Jacobsson B, Gonzalez-Martinez J, et al. Dissociation between in vitro and in vivo epileptogenicity in a rat model of cortical dysplasia. Epileptic Disorders. 2007 Mar;9(1):11–9.

31. Scantlebury MH, Ouellet PL, Psarropoulou C, Carmant L. Freeze lesion-induced focal cortical dysplasia predisposes to atypical hyperthermic seizures in the immature rat. Epilepsia [Internet]. 2004 Jun;45(6):592–600. Available from: http://www.ncbi.nlm.nih.gov/pubmed/15144423

32. Bell A, Jacobs KM. Early susceptibility for epileptiform activity in malformed cortex. Epilepsy Res. 2014;8(24):4017–8.

33. Lopantsev V, Avoli M. Laminar organization of epileptiform discharges in the rat entorhinal cortex in vitro. Journal of Physiology. 1998;(509.3):785–96.

34. Carcak N, Ozkara C. Seizures and Antiepileptic Drugs: From Pathophysiology to Clinical Practice. Curr Pharm Des. 2018 Feb 19;23(42):6376–88.

35. Ben-Ari Y, Cherubini E, Corradetti R, Gaiarsa JL. Giant synaptic potentials in immature rat CA3 hippocampal neurones. J Physiol [Internet]. 1989 Sep 1;416(1):303–25. Available from: https://onlinelibrary.wiley.com/doi/10.1113/jphysiol.1989.sp017762

36. Ben-Ari Y. Excitatory actions of GABA during development: The nature of the nurture. Vol. 3, Nature Reviews Neuroscience. 2002. p. 728–39.

37. Watanabe M, Fukuda A. Development and regulation of chloride homeostasis in the central nervous system. Vol. 9, Frontiers in Cellular Neuroscience. Frontiers Research Foundation; 2015.

38. Yamada J, Okabe A, Toyoda H, Kilb W, Luhmann HJ, Fukuda A. Cl- uptake promoting depolarizing GABA actions in immature rat neocortical neurones is mediated by NKCC1. Journal of Physiology. 2004 Jun 15;557(3):829–41.

39. Rivera C, Voipio J, Payne JA, Ruusuvuori E, Lahtinen H, Lamsa K, et al. The K+/Cl− co-transporter KCC2 renders GABA hyperpolarizing during neuronal maturation. Nature [Internet]. 1999 Jan;397(6716):251–5. Available from: https://www.nature.com/articles/16697

40. Defazio RA, Keros S, Quick MW, Hablitz JJ. Potassium-Coupled Chloride Cotransport Controls Intracellular Chloride in Rat Neocortical Pyramidal Neurons. 2000.

41. Wang C, Shimizu-Okabe C, Watanabe K, Okabe A, Matsuzaki H, Ogawa T, et al. Developmental changes in KCC1, KCC2, and NKCC1 mRNA expressions in the rat brain. Developmental Brain Research [Internet]. 2002 Nov;139(1):59–66. Available from: https://linkinghub.elsevier.com/retrieve/pii/S0165380602005369

42. Dzhala VI, Talos DM, Sdrulla DA, Brumback AC, Mathews GC, Benke TA, et al. NKCC1 transporter facilitates seizures in the developing brain. Nat Med. 2005 Nov;11(11):1205–13.

43. Liu R, Wang J, Liang S, Zhang G, Yang X. Role of NKCC1 and KCC2 in Epilepsy: From Expression to Function. Front Neurol. 2020;10(January):10–2.

44. Blauwblomme T, Dossi E, Pellegrino C, Goubert E, Iglesias BG, Sainte-Rose C, et al. Gamma-aminobutyric acidergic transmission underlies interictal epileptogenicity in pediatric focal cortical dysplasia. Ann Neurol. 2019 Feb 1;85(2):204–17.

45. Shimizu-okabe C, Tanaka M, Matsuda K. KCC2 was downregulated in small neurons localized in epileptogenic human focal cortical dysplasia. Epilepsy Res [Internet]. 2011;93(2–3):177–84. Available from: http://dx.doi.org/10.1016/j.eplepsyres.2010.12.008

46. Shimizu-okabe C, Okabe A, Kilb W, Sato K, Luhmann HJ, Fukuda A. Changes in the expression of cation-Cl À cotransporters , NKCC1 and KCC2 , during cortical malformation induced by neonatal freeze-lesion. Neurosci Res. 2007;59:288–95.

47. Wang T, Kumada T, Morishima T, Iwata S, Kaneko T, Yanagawa Y, et al. Accumulation of GABAergic Neurons, Causing a Focal Ambient GABA Gradient, and Downregulation of KCC2 Are Induced During Microgyrus Formation in a Mouse Model of Polymicrogyria. Cerebral cortex [Internet]. 2014;24(4):1088–101. Available from: http://www.pubmedcentral.nih.gov/articlerender.fcgi?artid=3948493&tool=pmcentrez&rendertype=abstract

48. Rosen GD, Sherman GF, Galaburda AM. Radial glia in the neocortex of adult rats: effects of neonatal brain injury. Developmental Brain Research. 1994;82(1–2):127–35.

49. Luhmann HL, Raabe K. Characterization of neuronal migration disorders in neocortical structures : I . Expression of epileptiform activity in an animal model. Epilepsy Res. 1996;(26):67–74.

50. Ragot A, Luhmann HJ, Dipper-Wawra M, Heinemann U, Holtkamp M, Fidzinski P. Pathology-selective antiepileptic effects in the focal freeze-lesion rat model of malformation of cortical development. Exp Neurol. 2021;343(May).

51. George Paxinos, Charles Watson. The Rat Brain in Stereotaxic Coordinates. Academic Press; 1986.

52. Ting JT, Daigle TL, Chen Q, Feng G. Acute brain slice methods for adult and aging animals: application of targeted patch clampanalysis and optogenetics. Methods Molecular Biology [Internet]. 2014;1183:1–21. Available from: http://link.springer.com/10.1007/978-1-4939-1096-0

53. Holtkamp D, Opitz T, Niespodziany I, Wolff C, Beck H. Activity of the anticonvulsant lacosamide in experimental and human epilepsy via selective effects on slow Na+ channel inactivation. Epilepsia. 2017;58(1):27–41.

54. Thöne J, Leniger T, Splettstösser F, Wiemann M. Antiepileptic activity of zonisamide on hippocampal CA3 neurons does not depend on carbonic anhydrase inhibition. Epilepsy Res. 2008;79(2–3):105–11.

55. Wahab A, Albus K, Heinemann U. Age- and region-specific effects of anticonvulsants and bumetanide on 4-aminopyridine-induced seizure-like events in immature rat

hippocampal-entorhinal cortex slices. Epilepsia [Internet]. 2011 Jan [cited 2013 Dec 15];52(1):94–103. Available from: http://www.ncbi.nlm.nih.gov/pubmed/21083847

56. Heuzeroth H, Wawra M, Fidzinski P, Dag R, Holtkamp M. The 4-Aminopyridine Model of Acute Seizures in vitro Elucidates Efficacy of New Antiepileptic Drugs. Front Neurosci. 2019;13(June):1–12.

57. D'Antuono M, Köhling R, Ricalzone S, Gotman J, Biagini G, Avoli M. Antiepileptic drugs abolish ictal but not interictal epileptiform discharges in vitro. Epilepsia. 2010 Mar;51(3):423–31.

58. Schwindt W, Burke M, Pillekamp F, Luhmann HJ, Hoehn M. Functional magnetic resonance imaging and somatosensory evoked potentials in rats with a neonatally induced freeze lesion of the somatosensory cortex. J Cereb Blood Flow Metab. 2004;24(12):1409–18.

59. dos Santos Heringer L, Rios Carvalho J, Teixeira Oliveira J, Texeira Silva B, de Souza Aguiar dos Santos DM, Martinez Martinez Toledo AL, et al. Altered excitatory and inhibitory neocortical circuitry leads to increased convulsive severity after pentylenetetrazol injection in an animal model of schizencephaly, but not of microgyria. Epilepsia Open. 2022 Sep 1;

60. Represa A. Why Malformations of Cortical Development Cause Epilepsy. Front Neurosci [Internet]. 2019;13(March):1–10. Available from: https://www.frontiersin.org/article/10.3389/fnins.2019.00250/full

61. Shain C, Ramgopal S, Fallil Z, Parulkar I, Alongi R, Knowlton R, et al. Polymicrogyria-associated epilepsy: A multicenter phenotypic study from the Epilepsy Phenome/Genome Project. Epilepsia. 2013 Aug;54(8):1368–75.

62. Herman AE, Galaburda AM, Fitch RH, Carter AR, Rosen GD, Neurology B, et al. Cerebral Microgyria , Thalamic Cell Size and Auditory Temporal Processing in Male and Female Rats. 1997;453–64.

63. Kamada T, Sun W, Takase KI, Shigetou H, Suzuki SO, Ohyagi Y, et al. Spontaneous seizures in a rat model of multiple prenatal freeze lesioning. Epilepsy Res. 2013 Aug;105(3):280–91.

64. Hablitz JJ, DeFazio RA. Altered Receptor Subunit Expression in Rat Neocortical Malformations. Epilepsia. 2005;41(s6):S82–5.

65. Zsombok A, Jacobs KM. Postsynaptic Currents Prior to Onset of Epileptiform Activity in Rat Microgyria. J Neurophysiol [Internet]. 2007;98(1):178–86. Available from: http://jn.physiology.org/cgi/doi/10.1152/jn.00106.2007

66. Awad PN, Sanon NT, Chattopadhyaya B, Ouardouz M, Gagn J, Duss S, et al. Reducing premature KCC2 expression rescues seizure susceptibility and spine morphology in atypical febrile seizures. Neurobiol Dis [Internet]. 2016; Available from: http://dx.doi.org/10.1016/j.nbd.2016.02.014

67. Gonzalez-Sulser A, Wang J, Motamedi GK, Avoli M, Vicini S, Dzakpasu R. The 4-aminopyridine in vitro epilepsy model analyzed with a perforated multi-electrode array. Neuropharmacology [Internet]. 2011;60(7–8):1142–53. Available from: http://dx.doi.org/10.1016/j.neuropharm.2010.10.007

68. Lillis KP, Kramer MA, Mertz J, Staley KJ, White JA. Pyramidal cells accumulate chloride at seizure onset. Neurobiol Dis. 2012 Sep;47(3):358–66.

69. Morris ME, Obrocea G v, Avoli M, Obrocea) G v. Extracellular K § accumulations and synchronous GABA-mediated potentials evoked by 4-aminopyridine in the adult rat hippocampus. Vol. 109, Exp Brain Res. Springer-Verlag; 1996.

70. Petit LF, Jalabert M, Buhler E, Malvache A, Peret A, Chauvin Y, et al. Normotopic cortex is the major contributor to epilepsy in experimental double cortex. Ann Neurol [Internet]. 2014 Sep [cited 2014 Oct 27];76(3):428–42. Available from: http://www.ncbi.nlm.nih.gov/pubmed/25074818

71. Christodoulou JA, Barnard ME, del Tufo SN, Katzir T, Whitfield-Gabrieli S, Gabrieli JDE, et al. Integration of gray matter nodules into functional cortical circuits in periventricular heterotopia. Epilepsy and Behavior. 2013 Nov;29(2):400–6.

72. Mai R, Tassi L, Cossu M, Francione S, lo Russo G, Garbelli R, et al. A neuropathological, stereo-EEG, and MRI study of subcortical band heterotopia. Neurology [Internet]. 2003 Jun 10;60(11):1834–8. Available from: https://www.neurology.org/lookup/doi/10.1212/01.WNL.0000065884.61237.24

73. Boulogne S, Pizzo F, Chatard B, Roehri N, Catenoix H, Ostrowsky-Coste K, et al. Functional connectivity and epileptogenicity of nodular heterotopias: A single-pulse stimulation study. Epilepsia. 2022 Apr 1;63(4):961–73.

74. Thom M, Martinian L, Parnavelas G, Sisodiya SM. Distribution of Cortical Interneurons in Grey Matter Heterotopia in Patients with Epilepsy. Vol. 45, Epilepsia. 2004.

75. Morimoto K, Sato H, Sato K, Sato S, Yamada N. BW1003C87, phenytoin and carbamazepine elevate seizure threshold in the rat amygdala-kindling model of epilepsy. Vol. 339, European Journal of Pharmacology. 1997.

76. Arzy S, Allali G, Brunet D, Michel CM, Kaplan PW, Seeck M. Antiepileptic drugs modify power of high EEG frequencies and their neural generators. Eur J Neurol. 2010 Oct;17(10):1308–12.

77. Wang-Tilz Y, Tilz C, Wang B, Pauli E, Koebnick C, Stefan H. Changes of seizures activity during rapid withdrawal of lamotrigine. Eur J Neurol [Internet]. 2005 Apr;12(4):280–8. Available from: https://onlinelibrary.wiley.com/doi/10.1111/j.1468-1331.2004.01101.x

78. Khateb M, Bosak N, Herskovitz M. The Effect of Anti-seizure Medications on the Propagation of Epileptic Activity: A Review. Vol. 12, Frontiers in Neurology. Frontiers Media S.A.; 2021.

79. Ben-Menachem E, Biton V, Jatuzis D, Abou-Khalil B, Doty P, Rudd GD. Efficacy and safety of oral lacosamide as adjunctive therapy in adults with partial-onset seizures. Epilepsia. 2007 Jul;48(7):1308–17.

80. Halász P, Kälviäinen R, Mazurkiewicz-Beldzińska M, Rosenow F, Doty P, Hebert D, et al. Adjunctive lacosamide for partial-onset seizures: Efficacy and safety results from a randomized controlled trial. Epilepsia. 2009;50(3):443–53.

81. Chung S, Sperling MR, Biton V, Krauss G, Hebert D, Rudd GD, et al. Lacosamide as adjunctive therapy for partial-onset seizures: A randomized controlled trial. Epilepsia. 2010;51(6):958–67.

82. Yang C, Yang Y, Peng Y, Zhang L, Yu D. Efficacy and safety of lacosamide in pediatric patients with epilepsy: A systematic review and meta-analysis. Epilepsy & Behavior. 2022 Sep;134:108781.

83. Behr C, Lévesque M, Ragsdale D, Avoli M. Lacosamide modulates interictal spiking and high-frequency oscillations in a model of mesial temporal lobe epilepsy. Epilepsy Res. 2015 Sep 1;115:8–16.

84. Lees G, Stöhr T, Errington AC. Stereoselective effects of the novel anticonvulsant lacosamide against 4-AP induced epileptiform activity in rat visual cortex in vitro. Neuropharmacology. 2006 Jan;50(1):98–110.

85. Niespodziany I, Leclère N, Vandenplas C, Foerch P, Wolff C. Comparative study of lacosamide and classical sodium channel blocking antiepileptic drugs on sodium channel slow inactivation. J Neurosci Res. 2013 Mar;91(3):436–43.

86. Errington AC, Stöhr T, Heers C, Lees G. The investigational anticonvulsant lacosamide selectively enhances slow inactivation of voltage-gated sodium channels. Mol Pharmacol. 2008 Jan;73(1):157–69.

87. Cho HY, Chuang TH, Wu SN. Evidence for Inhibitory Perturbations on the Amplitude, Gating and Hysteresis of A-Type Potassium Current, Produced by Lacosamide, a Functionalized Amino Acid with Anticonvulsant Properties. Int J Mol Sci. 2022 Feb 1;23(3).

88. Suzuki S, Kawakami K, Nishimura S, Watanabe Y, Yagi K, Scino M, et al. Zonisamide blocks T-type calcium channel in cultured neurons of rat cerebral cortex. Epilepsy Res. 1992;12(1):21–7.

89. Masuda Y, Noguchi H, Karasawa T. Evidence against a significant implication of carbonic anhydrase inhibitory activity of zonisamide in its anticonvulsive effects. Arzneimittelforschung. 1994 Mar;44(3):267–9.

90. Ito T, Hori M, Masuda Y, Yoshida K, Shimizu M. 3-Sulfamoylmethyl-l,2-benzisoxazole, a new type of anticonvulsant drug: Electroencephalographic profile. Jpn J Pharmacol [Internet]. 1979;29:30. Available from: https://linkinghub.elsevier.com/retrieve/pii/S0021519819668654

91. Masuda Y, Karasawa T, Shiraishi Y, Hori M, Yoshida K, Shimizu M. 3-sulfamoylmethyl-1,2-benzisoxazole,a new type of anticonvulsant drug. Pharmacological profile. Arzneimittelforschung. 1980;30:477–83.

92. Wada Y, Hasegawa H, Okuda H, Yamaguchi N. Anticonvulsant effects of zonisamide and phenytoin on seizure activity of the feline visual cortex. Brain Dev. 1990;12(2):206–10.

93. Akaike K, Tanaka S, Tojo H, Fukumoto S ichiro, Takigawa M, Imamura S ichi. Regional Accumulation of ^{14} C-zonisamide in Rat Brain during Kainic Acid-induced Limbic Seizures. Canadian Journal of Neurological Sciences / Journal Canadien des Sciences Neurologiques [Internet]. 2001 Nov 2;28(4):341–5. Available from: https://www.cambridge.org/core/product/identifier/S0317167100001554/type/journal_article

94. Keilin D, Mann T. Carbonic anhydrase. Purification and nature of the enzyme. Biochemical Journal [Internet]. 1940 Sep 1;34(8–9):1163–76. Available from: https://portlandpress.com/biochemj/article/34/8-9/1163/29451/Carbonic-anhydrase-Purification-and-nature-of-the

95. Shukralla AA, Dolan E, Delanty N. Acetazolamide: Old drug, new evidence? Epilepsia Open. John Wiley and Sons Inc; 2022.

96. Voipio J, Kaila K. GABAergic excitation and K+-mediated volume transmission in the hippocampus. Vol. 125, Brain Research. 2000.

97. Laxer KD, Hubesch B, Sappey-Marinier D, Weiner MW. Increased pH and Seizure Foci Inorganic Phosphate in Temporal Demonstrated by [31P]MRS. Vol. 33, Epilepsia. 1992.

98. Solntseva EI, Bukanova Y v., Skrebitsky VG. Effect of Protons on GABAA Receptors in Central Neurons of Various Types. Bull Exp Biol Med. 2020 Feb 1;168(4):419–22.

99. Yang F, Sun X, Ding Y, Ma H, Yang TO, Ma Y, et al. Astrocytic Acid-Sensing Ion Channel 1a Contributes to the Development of Chronic Epileptogenesis. Sci Rep. 2016 Aug 16;6.

100. Löscher W, Puskarjov M, Kaila K. Cation-chloride cotransporters NKCC1 and KCC2 as potential targets for novel antiepileptic and antiepileptogenic treatments. Neuropharmacology [Internet]. 2013;69:62–74. Available from: http://dx.doi.org/10.1016/j.neuropharm.2012.05.045

101. Rheims S, Represa A, Ben-Ari Y, Zilberter Y. Layer-Specific Generation and Propagation of Seizures in Slices of Developing Neocortex: Role of Excitatory GABAergic Synapses [Internet]. 2008. Available from: www.jn.org

102. Kourdougli N, Pellegrino C, Renko JM, Khirug S, Chazal G, Kukko-Lukjanov TK, et al. Depolarizing GABA contributes to glutamatergic network rewiring in epilepsy. Ann Neurol. 2017;

103. Sivakumaran S, Maguire J. Bumetanide reduces seizure progression and the development of pharmacoresistant status epilepticus. Epilepsia [Internet]. 2016 Feb;57(2):222–32. Available from: http://doi.wiley.com/10.1111/epi.13270

104. Hamidi S, Avoli M. KCC2 function modulates in vitro ictogenesis. Neurobiol Dis. 2015 Jul 1;79:51–8.

105. Ben-Ari Y. Neuro-archaeology: pre-symptomatic architecture and signature of neurological disorders. Trends Neurosci. 2008;31(12):626–36.

106. Javaheri S, Davis C, Rogers DH. Ionic Composition of Cisternal CSF in Acute Respiratory Acidosis: Lack of Effect of Large Dose Bumetanide. J Neurochem [Internet]. 1993 Oct;61(4):1525–9. Available from: https://onlinelibrary.wiley.com/doi/10.1111/j.1471-4159.1993.tb13648.x

107. Kahle KT, Barnett SM, Sassower KC, Staley KJ. Decreased seizure activity in a human neonate treated with bumetanide, an inhibitor of the Na+-K+-2Cl- cotransporter NKCC1. J Child Neurol. 2009;24(5):572–6.

108. Pressler RM, Boylan GB, Marlow N, Blennow M, Chiron C, Cross JH, et al. Bumetanide for the treatment of seizures in newborn babies with hypoxic ischaemic encephalopathy (NEMO): An open-label, dose finding, and feasibility phase 1/2 trial. Lancet Neurol. 2015 May 1;14(5):469–77.

109. Soul JS, Bergin AM, Stopp C, Hayes B, Singh A, Fortuno CR, et al. A Pilot Randomized, Controlled, Double-Blind Trial of Bumetanide to Treat Neonatal Seizures. Ann Neurol. 2021;89(2):327–40.

110. Cleary RT, Sun H, Huynh T, Manning SM, Li Y, Rotenberg A, et al. Bumetanide Enhances Phenobarbital Efficacy in a Rat Model of Hypoxic Neonatal Seizures. PLoS One. 2013 Mar 11;8(3).

111. Puskarjov M, Kahle KT, Ruusuvuori E, Kaila K. Pharmacotherapeutic targeting of cation-chloride cotransporters in neonatal seizures. Vol. 55, Epilepsia. Blackwell Publishing Inc.; 2014. p. 806–18.

112. Donovan MD, Schellekens H, Boylan GB, Cryan JF, Griffin BT. In vitro bidirectional permeability studies identify pharmacokinetic limitations of NKCC1 inhibitor bumetanide. Eur J Pharmacol. 2016;770:117–25.

113. Römermann K, Fedrowitz M, Hampel P, Kaczmarek E, Töllner K, Erker T, et al. Multiple blood-brain barrier transport mechanisms limit bumetanide accumulation, and therapeutic potential, in the mammalian brain. Neuropharmacology [Internet]. 2017;117:182–94. Available from: http://dx.doi.org/10.1016/j.neuropharm.2017.02.006

114. Johne M, Römermann K, Hampel P, Gailus B, Theilmann W, Ala-Kurikka T, et al. Phenobarbital and midazolam suppress neonatal seizures in a noninvasive rat model of birth asphyxia, whereas bumetanide is ineffective. Epilepsia. 2021;62(4):920–34.

115. Ben-Ari Y, Delpire E. Phenobarbital, midazolam, bumetanide, and neonatal seizures: The devil is in the details. Epilepsia [Internet]. 2021 Apr 3;62(4):935–40. Available from: https://onlinelibrary.wiley.com/doi/10.1111/epi.16830

116. Löscher W, Kaila K. Reply to the commentary by Ben-Ari and Delpire: Bumetanide and neonatal seizures: Fiction versus reality. Epilepsia. 2021;62(4):941–6.

117. Ben-Ari Y, Cherubini E. The GABA Polarity Shift and Bumetanide Treatment: Making Sense Requires Unbiased and Undogmatic Analysis. Cells. 2022;11(3):1–11.

118. Brandt C, Seja P, Töllner K, Römermann K, Hampel P, Kalesse M, et al. Bumepamine, a brain-permeant benzylamine derivative of bumetanide, does not inhibit NKCC1 but is more potent to enhance phenobarbital's anti-seizure efficacy. Neuropharmacology [Internet]. 2018 Dec;143:186–204. Available from: https://linkinghub.elsevier.com/retrieve/pii/S0028390818306774

119. Erker T, Brandt C, Töllner K, Schreppel P, Twele F, Schidlitzki A, et al. The bumetanide prodrug BUM5, but not bumetanide, potentiates the antiseizure effect of phenobarbital in adult epileptic mice. Epilepsia. 2016;57(5):698–705.

120. Hampel P, Römermann K, Gailus B, Johne M, Gericke B, Kaczmarek E, et al. Effects of the NKCC1 inhibitors bumetanide, azosemide, and torasemide alone or in combination with phenobarbital on seizure threshold in epileptic and nonepileptic mice. Neuropharmacology. 2021;185(December 2020).

121. O'Driscoll MC, Daly SB, Urquhart JE, Black GCM, Pilz DT, Brockmann K, et al. Recessive mutations in the gene encoding the tight junction protein occludin cause band-like calcification with simplified gyration and polymicrogyria. Am J Hum Genet [Internet]. 2010;87(3):354–64. Available from: http://dx.doi.org/10.1016/j.ajhg.2010.07.012

122. Jablonka JA, Binkowski R, Kazmierczak M, Sadowska M, Sredniawa W, Szlachcic A, et al. The Role of Interhemispheric Interactions in Cortical Plasticity. Front Neurosci. 2021 Jul 9;15.

123. Rema V, Ebner FF. Development/Plasticity/Repair Lesions of Mature Barrel Field Cortex Interfere with Sensory Processing and Plasticity in Connected Areas of the Contralateral Hemisphere. 2003.

124. Dick AS, Beharelle AR, Solodkin A, Small SL. Interhemispheric functional connectivity following prenatal or perinatal brain injury predicts receptive language outcome. Journal of Neuroscience. 2013 Mar 27;33(13):5612–25.

125. Wang DD, Knox R, Rolston JD, Englot DJ, Barkovich AJ, Tihan T, et al. Surgical management of medically refractory epilepsy in patients with polymicrogyria. Epilepsia. 2016 Jan 1;57(1):151–61.

126. Iurina E, Bailles E, Pintor L. Personality changes in patients with refractory epilepsy after surgical treatment: A systematic review. Seizure [Internet]. 2021 Feb 1;85:95–101. Available from: https://linkinghub.elsevier.com/retrieve/pii/S1059131121000030

127. Hristova K, Martinez-Gonzalez C, Watson TC, Codadu NK, Hashemi K, Kind PC, et al. Medial septal GABAergic neurons reduce seizure duration upon optogenetic closed-loop stimulation. Brain [Internet]. 2021 Jun 22;144(5):1576–89. Available from: https://academic.oup.com/brain/article/144/5/1576/6188981

128. Takeuchi Y, Harangozó M, Pedraza L, Földi T, Kozák G, Li Q, et al. Closed-loop stimulation of the medial septum terminates epileptic seizures. Brain [Internet]. 2021 Apr 12;144(3):885–908. Available from: https://academic.oup.com/brain/article/144/3/885/6121201

129. Hay M, Thomas DW, Craighead JL, Economides C, Rosenthal J. Clinical development success rates for investigational drugs. Nat Biotechnol [Internet]. 2014 Jan 9;32(1):40–51. Available from: http://www.nature.com/articles/nbt.2786

130. Seyhan AA. Lost in translation: the valley of death across preclinical and clinical divide – identification of problems and overcoming obstacles. Transl Med Commun. 2019 Dec;4(1).

Statutory declaration

I, Aliénor Ragot, by personally signing this document in lieu of an oath, hereby affirm that I prepared the submitted dissertation on the topic:

A study of the effects of antiepileptic drugs on the focal freeze lesion model: new insights on the pathophysiology of malformations of cortical development. /

Auswirkungen von Antiepileptika auf das fokale Freeze-Läsionsmodell: neue Erkenntnisse zur Pathophysiologie von Malformationen kortikaler Entwicklung,

independently and without the support of third parties, and that I used no other sources and aids than those stated.

All parts which are based on the publications or presentations of other authors, either in letter or in spirit, are specified as such in accordance with the citing guidelines. The sections on methodology (in particular regarding practical work, laboratory regulations, statistical processing) and results (in particular regarding figures, charts and tables) are exclusively my responsibility.

Furthermore, I declare that I have correctly marked all of the data, the analyses, and the conclusions generated from data obtained in collaboration with other persons, and that I have correctly marked my own contribution and the contributions of other persons (cf. declaration of contribution). I have correctly marked all texts or parts of texts that were generated in collaboration with other persons.

My contributions to any publications to this dissertation correspond to those stated in the below joint declaration made together with the supervisor. All publications created within the scope of the dissertation comply with the guidelines of the ICMJE (International Committee of Medical Journal Editors; http://www.icmje.org) on authorship. In addition, I declare that I shall comply with the regulations of Charité – Universitätsmedizin Berlin on ensuring good scientific practice.

I declare that I have not yet submitted this dissertation in identical or similar form to another Faculty.

The significance of this statutory declaration and the consequences of a false statutory declaration under criminal law (Sections 156, 161 of the German Criminal Code) are known to me.

Date Signature

Affidavit-Declaration of own contributions to the top-journal for a PhD degree

Aliénor Ragot contributed the following to the below listed publication:

Ragot A, Luhmann HJ, Dipper-Wawra M, Heinemann U, Holtkamp M, Fidzinski P.

Pathology-selective antiepileptic effects in the focal freeze-lesion rat model of malformation of cortical development. Exp Neurol. 2021 Sep; 343:113776. doi: 10.1016/j.expneurol.2021.113776. Epub 2021 May 29. PMID: 34058228.

Contributions in detail:

Conceptualization of the study and experiments:

Aliénor Ragot, Pawel Fidzinski, Uwe Heinemann

Heiko J Luhmann helped with the preparation of the protocol for the focal freeze lesion model and gave some technical tools.

Dipl.-Ing. Susanne Mueller, manager of the 7T Exp MRI lab helped with the technical conception of the MRI experiment

Execution of experiments:

All focal-freeze lesion surgeries were performed by Aliénor Ragot, as well as control of the state of the animals and habituation with occasional help from Lab technician Mandy Marbler Pötter

All electrophysiological experiments and IOS recording were performed by Aliénor Ragot

MRI recording were performed by Aliénor Ragot with occasional assistance from Susanne Mueller

Data Analysis:

All data and statistical analysis were performed by Aliénor Ragot- Matthias Dipper-Wawra helped and assisted with the use of custom-made MATLAB scripts for the analysis Intrinsic Optical Signal and SLE.

Preparation of all the figures of the article (Fig 1, 2, 3, 4, 5 and 6): Aliénor Ragot

Writing and revisions of the manuscript: Aliénor Ragot and Pawel Fidzinski

Editing of the manuscript: All authors

_____

Date, signature of first supervising university professor

_____

Date, signature of doctoral candidate

Excerpt from Journal Summary List

Journal Data Filtered By: **Selected JCR Year: 2019** Selected Editions: SCIE,SSCI
Selected Categories: **"NEUROSCIENCES"** Selected Category Scheme: WoS
Gesamtanzahl: 271 Journale

Rank	Full Journal Title	Total Cites	Journal Impact Factor	Eigenfactor Score
1	NATURE REVIEWS NEUROSCIENCE	42,809	33.654	0.055400
2	NATURE NEUROSCIENCE	62,933	20.071	0.144390
3	BEHAVIORAL AND BRAIN SCIENCES	9,395	17.333	0.008170
4	TRENDS IN COGNITIVE SCIENCES	27,705	15.218	0.036050
5	JOURNAL OF PINEAL RESEARCH	10,537	14.528	0.009430
6	NEURON	95,056	14.415	0.199640
7	ACTA NEUROPATHOLOGICA	21,908	14.251	0.040740
8	TRENDS IN NEUROSCIENCES	20,011	12.891	0.021220
9	Annual Review of Neuroscience	13,215	12.547	0.012740
10	MOLECULAR PSYCHIATRY	22,227	12.384	0.054730
11	Nature Human Behaviour	2,457	12.282	0.014190
12	BIOLOGICAL PSYCHIATRY	44,016	12.095	0.053910
13	BRAIN	53,282	11.337	0.067050
14	SLEEP MEDICINE REVIEWS	8,077	9.613	0.013000
15	Molecular Neurodegeneration	4,933	9.599	0.011840
16	PROGRESS IN NEUROBIOLOGY	12,791	9.371	0.011250
17	FRONTIERS IN NEUROENDOCRINOLOGY	4,491	9.059	0.007050
18	ANNALS OF NEUROLOGY	37,304	9.037	0.044120
19	NEUROSCIENCE AND BIOBEHAVIORAL REVIEWS	28,873	8.330	0.051900
20	Neurology-Neuroimmunology & Neuroinflammation	2,232	7.724	0.008400
21	NEUROPATHOLOGY AND APPLIED NEUROBIOLOGY	3,992	7.500	0.005960

Rank	Full Journal Title	Total Cites	Journal Impact Factor	Eigenfactor Score
22	Neurobiology of Stress	1,055	7.197	0.003840
23	NEUROPSYCHOPHARMACOLOGY	26,281	6.751	0.040680
24	npj Parkinsons Disease	662	6.750	0.002500
25	BRAIN BEHAVIOR AND IMMUNITY	16,285	6.633	0.028560
26	Brain Stimulation	6,537	6.565	0.015580
27	NEUROSCIENTIST	5,188	6.500	0.007220
28	Acta Neuropathologica Communications	4,070	6.270	0.014730
29	CURRENT OPINION IN NEUROBIOLOGY	14,959	6.267	0.028730
30	Alzheimers Research & Therapy	3,876	6.116	0.011650
31	Neurotherapeutics	4,998	6.035	0.009520
32	GLIA	14,220	5.984	0.017250
33	NEUROIMAGE	102,632	5.902	0.125360
34	Annual Review of Vision Science	601	5.897	0.003700
35	Molecular Autism	2,510	5.869	0.007450
36	Journal of Neuroinflammation	13,709	5.793	0.025870
37	Translational Stroke Research	2,274	5.780	0.004520
38	JOURNAL OF CEREBRAL BLOOD FLOW AND METABOLISM	19,492	5.681	0.024230
39	JOURNAL OF NEUROSCIENCE	167,114	5.673	0.181170
40	BRAIN PATHOLOGY	5,308	5.568	0.007020
41	Translational Neurodegeneration	1,030	5.551	0.002790
42	NEURAL NETWORKS	14,065	5.535	0.018910
43	PAIN	37,753	5.483	0.035730

Selected JCR Year: 2019; Selected Categories: "NEUROSCIENCES"

Rank	Full Journal Title	Total Cites	Journal Impact Factor	Eigenfactor Score
44	Multiple Sclerosis Journal	11,792	5.412	0.019460
45	BIPOLAR DISORDERS	4,838	5.410	0.006610
46	Dialogues in Clinical Neuroscience	3,842	5.397	0.005280
47	Biological Psychiatry-Cognitive Neuroscience and Neuroimaging	1,361	5.335	0.005880
48	NEUROBIOLOGY OF DISEASE	17,200	5.332	0.023770
49	Brain Connectivity	2,431	5.263	0.005180
50	Journal of Parkinsons Disease	2,244	5.178	0.005810
51	CEREBRAL CORTEX	30,815	5.043	0.056030
52	Developmental Cognitive Neuroscience	3,177	4.966	0.010180
53	CEPHALALGIA	11,053	4.868	0.011970
54	NEUROPSYCHOLOGY REVIEW	3,114	4.840	0.004050
55	SLEEP	22,296	4.805	0.024610
56	JOURNAL OF HEADACHE AND PAIN	3,898	4.797	0.007600
57	PSYCHONEUROENDOCRINOLOGY	19,287	4.732	0.027100
58	JOURNAL OF NEUROSCIENCE RESEARCH	13,098	4.699	0.010490
59	EXPERIMENTAL NEUROLOGY	20,154	4.691	0.020070
60	Molecular Brain	2,785	4.686	0.006510
61	Current Neuropharmacology	4,178	4.668	0.006280
62	JOURNAL OF PAIN	10,887	4.621	0.015040
63	JOURNAL OF PHYSIOLOGY-LONDON	50,045	4.547	0.037090
64	EUROPEAN JOURNAL OF NEUROLOGY	11,015	4.516	0.017330
65	MOLECULAR NEUROBIOLOGY	15,297	4.500	0.031350

Selected JCR Year: 2019; Selected Categories: "NEUROSCIENCES"

Print copy of the publication

https://doi.org/10.1016/j.expneurol.2021.113776

https://doi.org/10.1016/j.expneurol.2021.113776

https://doi.org/10.1016/j.expneurol.2021.113776

https://doi.org/10.1016/j.expneurol.2021.113776

https://doi.org/10.1016/j.expneurol.2021.113776

https://doi.org/10.1016/j.expneurol.2021.113776

https://doi.org/10.1016/j.expneurol.2021.113776

https://doi.org/10.1016/j.expneurol.2021.113776

https://doi.org/10.1016/j.expneurol.2021.113776

https://doi.org/10.1016/j.expneurol.2021.113776

https://doi.org/10.1016/j.expneurol.2021.113776

https://doi.org/10.1016/j.expneurol.2021.113776

https://doi.org/10.1016/j.expneurol.2021.113776

Curriculum Vitae

My curriculum vitae does not appear in the electronic version of my paper for reasons of data protection

My curriculum vitae does not appear in the electronic version of my paper for reasons of data protection

Publication list

1. **Ragot A**, Luhmann HJ, Dipper-Wawra M, Heinemann U, Holtkamp M, Fidzinski P. Pathology-selective antiepileptic effects in the focal freeze-lesion rat model of malformation of cortical development. Exp Neurol. 2021 Sep;343:113776. doi: 10.1016/j.expneurol.2021.113776. Epub 2021 May 29. PMID: 34058228.
   Impact factor (2021):5.33

2. Schlabitz S, Monni L, **Ragot A**, Dipper-Wawra M, Onken J, Holtkamp M, Fidzinski P.
   Spatiotemporal Correlation of Epileptiform Activity and Gene Expression *in vitro*. Front Mol Neurosci. 2021 Mar 30;14:643763. doi: 10.3389/fnmol.2021.643763. PMID: 33859552; PMCID: PMC8042243.
   Impact factor (2021):6.261

3. **Ragot A**, Pietropaolo S, Vincent J, Delage P, Zhang H, Allinquant B, Leinekugel X, Fischer A, Cho YH.
   Genetic deletion of the Histone Deacetylase 6 exacerbates selected behavioral deficits in the R6/1 mouse model for Huntington's disease. Brain Behav. 2015 Sep;5(9):e00361. doi: 10.1002/brb3.361. Epub 2015 Jun 24. PMID: 26445700; PMCID: PMC4589808. Impact factor (2021):3.405

Acknowledgments

This project was funded by the DESIRE Consortium, an FP7-HEALTH funded European project. The DESIRE project focused on Development and Epilepsy – Strategies for Innovative Research to Improve Diagnosis, Prevention and Treatment In children with Difficult-to-treat Epilepsy (https://www.epilepsydesireproject.eu/).
Thank you to all members of the consortium, the annual meetings of the project were a great source of knowledge and inspiration. The sincere and open international collaboration that happened in this project is what Science should always be about.

This study was based on an idea of Prof Uwe Heinemann (†) in collaboration with my supervisors PD Dr. med. Pawel Fidzinski and Prof. Dr. Martin Holtkamp.
I thank Prof Heinemann for his teachings and advice at the beginning of this project, the field of Epilepsy and myself owe him a great debt. He was also a very kind man who took the time to help every student that pushed the door of his office. I was lucky to be one of those students.

To my supervisor Martin Holtkamp, thank you for giving me a position in your team and encouraging me through this long process. As a biologist in a research team of neurologists, thank you for passing on your knowledge and experience of the care of patients with epilepsy.

To my supervisor Pawel Fidzinski, thank you for bringing me into the team when we could count its members on one hand with a couple of fingers left. Thank you for teaching me and pushing me to try new techniques. Your philosophy “try it first by yourself and when you’re completely stuck, I’ll show you” has definitely made me more adventurous and luckily, nothing exploded in the lab. I have learned a great deal during this PhD, and I thank you for your help and supervision.

Thank you, Matthias, for your help and advice especially on the analysis of the intrinsic signal recording. It’s always a pleasure working with you.

Thank you to Mandy, who was such a precious help in the lab and made my daily life in the lab some much easier through her work and brighter by her presence.

Thank you to all the bachelor, master and medical students who did internships in the lab under my supervision: Jonas, Yser, Alexandros, Sophie, Angel, Christian. Your curiosity and intelligence were a tonic, and it was lovely to get to know such nice people and promising scientists.

À Lucille, merci pour ton amitié depuis les bancs de Bordeaux 2 jusqu'à Berlin, ta finesse et ton intelligence sont une source d'inspiration. Merci d'avoir été toujours là, j'espère te voir bientôt et entendre de nouveau ton rire lumineux.

To Tiziano and Sharon, thank you for being there for me during the ups and downs of this long PhD, my life in Berlin without you both would have been flavourless.

À Anne, merci pour ton amitié qui m'a accompagnée presque aussi loin que je me souvienne, et merci de m'accueillir dans cette phase de transition. Je finis ce texte dans ton salon.

À mes parents et mes sœurs, merci d'avoir toujours cru en moi et de m'avoir offert un soutien inconditionnel pendant ces années. Je ne peux exprimer la force et la chaleur que vous m'avez apportées. Grâce à vous je n'ai jamais eu froid, même lors de mes longs hivers berlinois.

To Gbolahan, mo nifẹ rẹ, o ṣeun fun ohun gbogbo.